Energy & Buildings 261 (2022) 111941

Contents lists available at ScienceDirect

Energy & Buildings

journal homepage: www.elsevier.com/locate/enb

Seasonal adaptation of VRF HVAC model calibration process to a mediterranean climate

José Eduardo Pachano [a], Antonis Peppas [b], Carlos Fernández Bandera [a,*]

[a] School of Architecture, University of Navarra, 31009 Pamplona, Spain
[b] School of Mining and Metallurgical Engineering, National Technical University of Athens (NTUA), Athens, Greece

ARTICLE INFO

Article history:
Received 9 November 2021
Revised 19 January 2022
Accepted 10 February 2022
Available online 14 February 2022

Keywords:
Building energy models (BEM)
HVAC
Calibration
Variable refrigerant flow (VRF)
Energy simulation
Genetic algorithm
Air conditioning (AC)

ABSTRACT

Today, Building Energy Models (BEM) have become essential in regulatory compliance calculations, the correct assessment of it's Air Conditioning (AC) systems is critical for the reduction of the performance gap between BEMs and reality and increase the accuracy of evaluating buildings energy performance and it's systems efficiency. Given that multi-split Variable Refrigerant Flow (VRF) systems have grown in the market in recent years becoming a particular trending solution to achieve building indoor comfort; the present paper focus on technical issues when modelling such VRF systems inside EnergyPlus, a white-box simulation environment, especially regarding the effects weather conditions have on the behaviour of VRF systems and it's correlation with the AC system performance curves. The study performs an empirical validation of an optimization-based calibration methodology assessing multiple levels: average interior temperature of the different building spaces and electric energy consumption from VRF outdoor unit. It is performed using fifteen minute time-step seasonal data obtained from a fully operational building located in a typical Mediterranean climate (Greece), adjusting the parameter and curve values of the VRF system using a genetic NGSA-II algorithm (Jeplus software) for both summer and winter conditions. The generated BEM captures the building's hourly performance for summer conditions using 1717 hours to fit into international standards. Complying with the requirements of the American Society of Heating, Refrigerating and Air-Conditioning Engineers (ASHRAE) Guidelines 14-2002 for hourly energy consumption, reaching an NMBE $\leqslant \pm 10\%$,Cv(RMSE) $\leqslant 30\%$ and R2 $\geqslant 75\%$ while keeping indoor temperatures on every room with a RMSE $\leqslant 1\ ^{\circ}C$. The resulting BEM proved stable during the 2077 hours of it's summer evaluation period, fitting into the new unseen weather and building operation conditions of 2020 which can be considered a step forward in the area of calibrating white box models. While for winter conditions the study demonstrates the value of the calibration methodology while presenting the importance of weather influence on VRF systems. Using a total of 802 hours the applied technology greatly improves the results from the baseline model, reaching a partially calibrated BEM model for winter. Which reinforces the fact that regardless of how good a baseline model is, building operating conditions and weather may will always generate a design/performance gap and therefore the calibration of a BEM is unavoidable.

© 2022 The Author(s). Published by Elsevier B.V. This is an open access article under the CC BY-NC-ND license (http://creativecommons.org/licenses/by-nc-nd/4.0/).

1. Introduction

Multi-split Variable Refrigerant Flow (VRF) Air Conditioning (AC) systems can meet the heating and/or cooling demand, depending of the system's pipe configuration, from different building areas occupying seemingly less space. Their simpler installation procedure allows multiple indoor units are mounted in the building and connected to just a few outdoor units [1]. When their installation, operation and maintenance cost is compared against any other traditional Heating Ventilation and Air Conditioning (HVAC) systems, VRF configurations are usually more economical being able to maintain indoor temperature conditions while decreasing energy consumption due to the possibility of their individual control mode [2]. For these reasons, the application of VRF as an HVAC solution has become particularly trending in current years, gaining more and more space in the market for small and medium sized commercial and residential buildings demonstrating it's flexibility [3]. More so since, as Gilani et. al. states [4], VRF systems can work in conjunction with other renewable technologies

* Corresponding author.
E-mail addresses: jpachano@unav.es (J.E. Pachano), cfbandera@unav.es (C.F. Bandera).

https://doi.org/10.1016/j.enbuild.2022.111941
0378-7788/© 2022 The Author(s). Published by Elsevier B.V.
This is an open access article under the CC BY-NC-ND license (http://creativecommons.org/licenses/by-nc-nd/4.0/).

Nomenclature

Abbreviations

AHU	Air Handling Unit
ASHRAE	American Society of Heating, Refrigerating and Air-Conditioning Engineers
BEM	Building Energy Model
BMS	Building Management System
CIBSE	Chartered Institution of Building Services Engineers
Cv(RMSE)	Coefficient of Variation of Mean Square Error
DoE	Department of Energy
DHW	Domestic Hot Water
DR	Demand Response
DX	Direct Expansion
ECMs	Energy Conservation Measures
EU	European Union
FCU	Fan Coil Unit
FEMP	Federal Energy Management Program
HP	Heat Pump
HPWH	Heat Pump Water Heater
HVAC	Heating Ventilation Air Conditioning
IEA	International Energy Agency
IPMVP	International Performance Measurement and Verification Protocol
M&V	Measuring and Verification
MAE	Mean Absolute Error
MPC	Model Predictive Control
NMBE	Normalized Mean Bias Error
NSGA-II	Non-Dominated Sorting Genetic Algorithm
R^2	Spearman's Rank Correlation Coefficient Square
RMSE	Root Mean Square Error
SABINA	SmArt BI-directional multi eNergy gAteway
Temp.	Temperature
TZ	Thermal Zone
VRV	Variable Refrigerant Volume
VRF	Variable Refrigerant Flow
$\Delta\Theta$	Temperature Differential Range
°C	Celsius degrees
kW	Kilowatt
kWh	Kilowatt per hour
mm	Millimeters
m/s	Meters per second
m^3/h	Cubic meters per hour
Pa	Pascals
W	Watts
Wh	Watt per hour
%	Percentage
° or deg	Decimal degrees

like photo-voltaic panels (PV). Which not only demonstrates this is an adaptable HVAC system, it opens the door for its usage in thermal mass activation, Demand Response (DR), Model Predictive Control (MPC) or other potential energy saving strategies. Given that Heating, Ventilation and Air Conditioning (HVAC) systems installed inside a structure can account for approximately 50 to 60% of the total energy consumed by the building [5], it is no surprise that studies like the ones from Lee et. al. [6], Aynur et. al. [7] and Yu et. al. [8] focus on VRF performance improvement, comparison of this system with other commonly used HVAC solutions like Variable Air Volume (VAV) and optimizing VRF energy savings.

The fact is that in terms of global final energy buildings consumption can reach approximately 32%, when assessing their impact in worldwide primary energy consumption their influence increases to 40% [9,10], this corresponds to 19% of global carbon emissions [11]. The impact of HVAC systems in the global energy consumption scenario could be estimated to around 20% [5]. Which turns both the building and it's HVAC system into crucial participants in the global energy consumption scenario. This is why many countries have established mandatory energy studies in all building projects, be that new or retrofit, in order to increase energy performance, reduce CO_2 emissions, and improve maintenance costs [12]. After all, as the Report of the Intergovernmental Panel on Climate Change (IPCC) suggest, the execution of building retrofits and the application of different Energy Conservation Measures (ECM) could achieve worldwide building energy savings from 50% to 90% [13] and therefore assessing correctly building energy performance becomes key to develop the right strategies to optimize energy savings, find new solutions and avoid wasting resources. Assessing the energy behaviour of any site and capturing it's HVAC performance is a challenge comprised of multiple uncertainties and assumptions, where we estimate parameter values of the multiple passive and active systems in an attempt to emulate reality [14] in order to reduce the gap between the results obtained from the simulated Building Energy Model (BEM) and reality.

To achieve this, the Measure and Verification (M&V) Guidelines [15], the International Performance Measurement and Verification Protocol (IPMVP) [16] and The American Society of Heating, Refrigerating and Air-Conditioning Engineers (ASHRAE) Guideline 14-2002 [17], have set the procedures to execute these energy consumption assessments and the calibration of both: buildings and their HVAC equipment. Using IPMVP as a reference, the are four different options to assess energy performance depending of the boundary level of the study. While options A and B focuses on obtain the performance of a single system or component in laboratory conditions [18], or focusing solely on optimizing the behaviour of a single equipment [19] or a particular HVAC loop [20,21] by limiting the measurement boundary to evaluate their performance in "isolation" from the rest of the building. IPMVP last two options treat the assessment of building energy performance as a whole, evaluating the building and it's systems by the use of utility meters as Option C states, or developing a Building Energy Model (BEM) in a simulation environment to capture the building's heat and energy dynamics under Option D. This last option is a powerful non-intrusive tool that can identify issues in the building's multiple systems, from envelope to HVAC behaviour, validating energy savings for future Energy Conservation Measures (ECM) deployments [22], or assessing multiple HVAC configurations [23] to design and/or commission the building's systems [24]. The aim of Option D is to produce a calibrated BEM that accurately represents the building's energy performance, a model stable through different time periods that works under various internal operational and external environmental factors [25–27].

These environmental factors are extremely important in the case of a VRF unit. Studies like the one of Zhang et al. evaluate the performance of a variable multiple AC system under different part load ratios for hot summer and cold winter conditions [28]. This puts the equipment in the best possible operational outside conditions, but in the case of a typical Mediterranean climate where we have hot summer conditions but mild winters the equipment efficiency performs quite differently under non optimal out-

side conditions. Which is why it is important to treat heating and cooling systems independently as Guyot et. al. suggests [29], finding the right solution that establishes both: how the equipment operates and how it correctly distributes it's heating and cooling energy into the building [30,31] to meet indoor conditions.

In essence, capturing a building's energy performance requires a multi-level benchmark process that ensures that the energy consumed is in accordance to the indoor temperature behavior, linking comfort conditions and building's cooling/heating demand to the HVAC consumption in the same monthly or hourly resolution. In other words, cross checking the energy consumption of the different building HVAC systems with the Thermal Zones (TZ) interior temperatures, the building's indoor climate [32,33]. It is here that Variable Refrigerant Flow (VRF) systems can be particularly helpful, as described by Yun and Song [34], EnergyPlus VRF models require the introduction of detailed performance and energy consumption curves which define the behaviour of the equipment, taking into account both indoor temperatures and outdoor conditions to establish the equipment's energy output. Which is why many studies, like Kang et. al. [35], Yin et. al. [36] and Hydeman et. al. [37,38] focuses on obtaining the equipment performance curves to calibrate the HVAC energy outputs. Once this is achieved other influential parameters may be optimized, for example: T. Hong et. al. [39], J. Chen et. al. [40], Chong and Menberg [41], and Lim and Zhai [42] make use of set-point values and the equipment's Coefficient of Performance (COP) to calibrate the HVAC performance.

The main objective of this study is to validate the following parameter calibration methodology in H2Susbuild VRF HVAC system, a real test site building located in Lavrio-Greece under normal day-to-day operation. Acquiring a white-box simulation BEM that complies to hourly international standards in a multilevel benchmark: indoor temperature and electric consumption. Demonstrating why, regardless of how good a baseline model is, boundary conditions make it clear it is key to always perform a calibration of any BEM, and bringing into discussion the importance of weather not only as a building stressing factor, but as an actor in determining VRF equipment behaviour and efficiency. The following study was developed using 2019-20 measurement campaigns setting multiple sensors and a weather station on-site to obtain the test site weather on location, building's indoor temperatures and electric consumption; relying on both: the Building Management System (BMS) data collection capabilities and minimum site sensor deployment for establishing the HVAC system operation.

The novelty presented in this study is the application and validation of a multi-level HVAC calibration methodology performed in EnergyPlus white-box simulation environment of a real test site, where VRF performance curves and HVAC component parameters are optimized simultaneously capturing the VRF system behaviour using only 2519 hours of fifteen minute time-step data, adapting the BEM's HVAC system for summer and winter conditions of a typical Mediterranean climate (Greece). The resulting BEM proved stable during the 2077 hours of it's summer evaluation period, fitting into the new unseen weather and building operation conditions of 2020.

The structure of the following paper is established as: Section 2 presents the calibration methodology and it's principles applied to the current test site. Section 3 describes the building, it's HVAC systems and the generation of the baseline BEM that will undergo the calibration process, while including considerations regarding data quality required for calibrating the models. Section 4 discuss the results obtained for this case study for both: training and checking periods, illustrating the benefits of the calibrated BEM when compared against a state of the art baseline BEM. Furthermore it demonstrates the importance that weather conditions have when optimizing VRF performance curves and parameters on on-site installed equipment. Finally, Section 5 lists the conclusions obtained from this practical validation and outlines future studies on the application of this methodology and the use of this calibrated BEMs.

2. Calibration methodology

The successful empirical application of this inverse calibration methodology used to obtain building and HVAC equipment parameter values within EnergyPlus white-box simulation environment has been fully detailed and validated in previously published studies by the authors [43,44]. The objective of the following subsections is to briefly describe the methodology and the benchmark framework under which the models would be assessed, focusing on the adaptations performed to the current case study proving the methodology's flexibility to different HVAC equipment schemes.

2.1. Methodology description

Indoor temperatures are the result of the building's energy balance, it is the indoor space response to a variety of external (weather) and internal (loads) factors. For the building to serve it's occupants, it's interior spaces need to achieve comfort conditions, which are established in terms of temperature and air quality. This results in a correlation between it's indoor climate (temperature) to the energy demanded by the different spaces and supplied by the building's HVAC system. The first problem lies in faithfully establishing the effects of this system in relation to all the other systems that are involved in building thermodynamics. One way of achieving this is to separate the calibration process into multiple steps and addressing first the envelope system, a process demonstrated by the authors previously [44]. For once the envelope has been calibrated, the amount of energy gained and lost through it is established, and therefore we can access directly to the energy demand of the building (Annex 49 [45,46]).

In other words, after establishing the indoor occupancy related loads like lighting and power, any further changes in indoor temperature; be by gaining it, losing it or maintaining it are the result of the HVAC system influence alone. As Fig. 2 displays, indoor temperature is the result of heating or cooling energy acting into the different building spaces. Energy that can only be introduced into the building environment by the means of expending a resource as fuel, in the particular case of this study, electric energy. As such, we can establish that indoor temperatures are correlated to HVAC electric consumption through the means of the equipment thermal performance.

Usually the way we would calibrate this building would be by trying to match the 3 aspects of the energy balance: indoor climate, thermal energy and electric energy. But in the case of H2SusBuild particular HVAC system, a two-pipe variable refrigerant flow system, there is no simple way to measure the thermal energy introduced and distributed into the complicated HVAC distribution system. Fig. 2 displays the characterization of this particular building behaviour to capture its thermal dynamics must rely solely on the correlation between two key agents in building energy simulation: indoor temperature and electric consumption.

The initial step to perform the calibration process shown in Fig. 1,is to generate inside EnergyPlus white-box simulation environment a baseline BEM that incorporates as much information from the actual test site building and it's different systems, aiming to represent as closely as possible real on-site conditions. [32] The objective is to generate the best possible simulation model based on all available information from the building and its sub systems. A BEM detailing the building and it's HVAC system whose

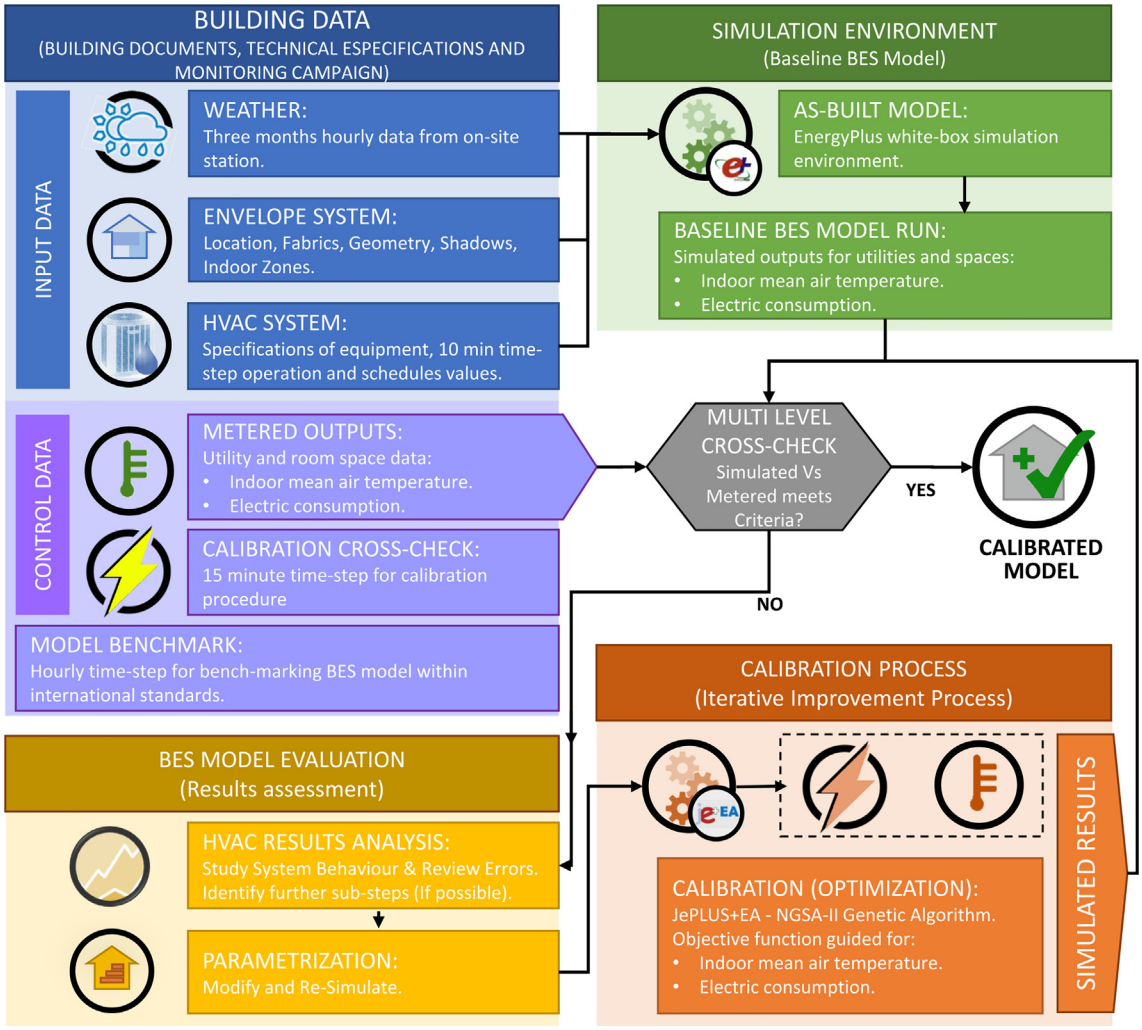

Fig. 1. Overview of Calibration Methodology.

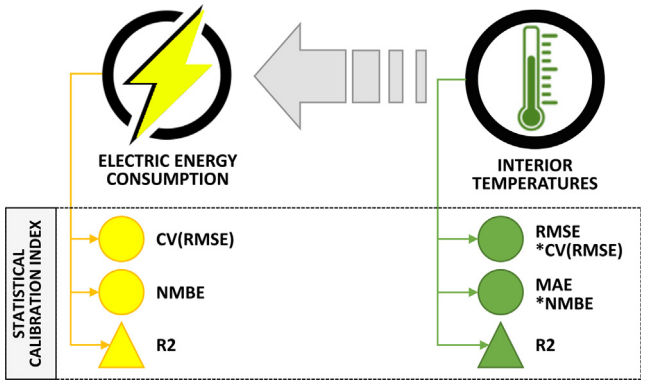

Fig. 2. Conditions required for the Calibration Process: interior temperatures and electric consumption. Simulated results must fit both levels. (Note*: The NMBE and Cv(RMSE) indices for indoor temperature are only displayed to execute comparisons with existing literature.).

parameter values are based on information obtained from the building's and equipment's technical documentation. The resulting BEM contains: the building's previously calibrated envelope, it's geographical location, shadowing, indoor spaces areas and volumes, conditioned and unconditioned area classification, constructions and materials, any required external or internal loads, and the detail model of it's HVAC system.

The calibration of a BEM is an optimization iterative process, where some parameter values are shifted until a solution, or group of solutions, that satisfies a given set of constrains are found. In other words, it is a continuous benchmark cycle and as any other benchmark process, data is a major factor in the process. As Fig. 1 illustrates, the data obtained from the sensors installed inside the building can be classified into input data and control data depending on how it will be used inside the simulation environment. Input data refers to a stream of measurable sensor data that would be likely used to stress or stimulate the simulation environment during the calibration process, for example: weather conditions, temperature set-points, equipment operation, air flow, and others shown in Table 1. While Control data is a separate stream that is used in the comparison between BEM simulated results with their measured counterparts, like: indoor room temperature and electric energy consumption, to benchmark the quality of the calibration process on the selection of the different parameter values.

This optimization process is run on jEPlus+EA software. jEPlus is an EnergyPlus simulation environment tool aimed to perform complex parametric simulations [47]. The additional subroutine set in jEPlus+EA introduces in the simulation environment a particular second generation multi-objective Non Sorting Genetic Algorithm

Table 1
List of measurement sensors commonly used in data driven BEMs with a VRF HVAC system.

Measurement	*Units*
Weather :	
Outdoor Dry Bulb Temperature	°C
Outdoor Relative Humidity	%
Ground Temperature	°C
Diffuse Radiation	W/m^2
Global Horizontal Radiation	W/m^2
Atmospheric Pressure	Pa
Wind Direction	deg
Wind Speed	m/s
Precipitation	mm
IndoorClimate :	
Interior Room Temperature by TZ	°C
HVACSystem :	
Equipment ON/OFF status	1/0
ElectricConsumption :	
Lighting Electric Energy Consumption	Wh
Outlet Electric Energy Consumption	Wh
HVAC Electric Energy Consumption	Wh
HVAC Electric Power Rate Consumption	W

(NSGA-II) into jEPlus platform [48]. In this way a set of objective functions can be established in terms of the building's interior temperatures and the equipment electric consumption that will guide the behaviour of the algorithm in the selection of the parameter values that best fit the BEM simulation results when comparing them against the real test site measured data.

When developing the baseline BEM model into the calibration framework, an initial result analysis is performed prior the parametrization process. The results of this initial run allows to establish the calibration strategy, in other words, select the parameters that undergo the calibration process and group similar components and/or HVAC equipment to reduce the solution search space. The resulting key parameters selected and the grouping of HVAC elements used in this study are tabulated in Section 4.1, the process is performed separately for winter and summer conditions, in two steps, as it halves the size of the parameter list and therefore the solution search space, focusing the calibration into finding the best parameter values for the local seasonal conditions.

As explained before in the case of the VRF system deployed in the case study building, there are no measurements for heating or cooling energy obtained from the refrigerant flow pipes. Therefore, inside the simulation environment heating and cooling energy is established through VRF capacity parameters and the equipment performance curves. To state a BEM has reached calibration, the obtained solution must satisfy both: indoor temperature and electric consumption as displayed on Fig. 2, since doing so would indirectly satisfy heating and cooling energy and it will effectively capture the building's VRF system behaviour.

The application of this multi-step calibration process is flexible and versatile, it can be applied to a variety of different building systems and/or HVAC equipment to describe their behaviour. For the BEM to reach calibration status, the results obtained from the simulation must meet an international standard on multiple benchmark levels. In this particular case, since the simulated VRF system correlates indoor climate to electric energy consumption, a two level benchmark that focuses on these results would be considered enough to satisfy calibration criteria established by international standards.

2.2. Calibration statistical indices

The threshold under which a BEM is usually dubbed as calibrated is determined by different international protocols and standards applied depending on the type, or level, of benchmark executed. The American Society of Heating, Refrigerating and Air Conditioning Engineers (ASHRAE) Guideline 14 [17] and the International Performance Measurement and Verification Protocol (IPMVP) [16] are used to evaluate the BEM's energy performance. To do so, the aforementioned standards make use of the normalized mean bias error (NMBE) shown in Eq. 1, and the coefficient of variation of the root mean square error (CvRMSE) shown in Eq. 2.

$$NMBE = \frac{1}{\overline{m}} \cdot \frac{\sum_{i=1}^{n}(m_i - s_i)}{n-p} \cdot 100(\%) \tag{1}$$

$$CV(RMSE) = \frac{1}{\overline{m}} \cdot \sqrt{\frac{\sum_{i=1}^{n}(m_i - s_i)^2}{n-p}} \cdot 100(\%) \tag{2}$$

While the Chartered Institution of Building Services Engineers (CIBSE), on it's publication Operation Performance TM-63: Building performance modelling and calibration for evaluation of energy in-use [49], cites the studies of Royapoor and Roskilly [50]; which in conjunction with the German standard VDI-6020:2002 [51] provide a framework to evaluate building's indoor temperature performance. They make use of the mean absolute error (MAE) shown in Eq. 3, and the root mean square error (RMSE) displayed in Eq. 4, to execute the comparison between simulated BEM results and their measured counterparts.

$$MAE = \frac{\sum_{i=1}^{n}|m_i - s_i|}{n}, \tag{3}$$

$$RMSE = \sqrt{\frac{\sum_{i=1}^{n}(m_i - s_i)^2}{n}} \tag{4}$$

Taking into account that a BEM performance evaluation, or how well a BEM fits into reality, is established by using of at least one bias index in company of one goodness-of-fit index [52]. In other words, measuring the error distance, or residual vector shown in Eqs. (1)–(4), while comparing the shape likelihood between the simulated results curve and the one belonging to real measured data. To achieve this we take note of ASHRAE Guideline 14 [17] and IMPVP [16] recommendation, applying the square of the Pearson correlation coefficient (R^2) shown in Eq. 5 as a measure for this goodness-of-fit quality in all benchmark levels.

$$R^2 = \left(\frac{\sum_{i=1}^{n}(m_i - \overline{m}).(s_i - \overline{s})}{\sqrt{\sum_{i=1}^{n}(m_i - \overline{m})^2 . \sum_{i=1}^{n}(s_i - \overline{s})^2}} \right)^2 \tag{5}$$

where:

$\overline{s}$ = the mean of simulated values
$\overline{m}$ = the mean of measured values
s_i = the simulated value
m_i = the measured value
p = 1 (According to BEM M&V methodology)
n = the number of data points

The values for the different uncertainty index threshold involved in this multi-level evaluation of simulated BEM results for hourly electric energy consumption and interior room temperature are shown in Table 2. This limit values have been developed for a stream of yearly data, since there is an inherent challenge with projects involving real "in operation" test facilities to obtain such a stream of healthy, valid data; we aim to reach these standardized values with as much data as possible. In other words, we aim to calibrate the building and it's system parameter values with less amount of data than the yearly one required by the standard, generating a BEM that captures the behaviour of the building

Table 2
Limit values for uncertainty hourly error indices used in model calibration.

HourlyIndex	Energy Consumption		Indoor Temperature
	ASHRAE	*IPMVP*	*CIBSE VDI – 6020*
MAE (°C)	–	–	≤2.0
RMSE (°C)	–	–	≤1.5
NMBE (%)	⩽±10	⩽±5	–
CV(RMSE) (%)	≤30	≤20	–
R2 (%)	⩾75	⩾75	⩾75

and it's systems and is stable when checked under new unseen data in a different time period than the one used on it's calibration.

3. Case study description

Located in Lavrion-Greece at an altitude above sea level of 26 m, H2SusBuild is a nearly zero CO_2 emissions light construction living lab that is part of the Lavrion Technological and Cultural Park (LTCP) and is run by the National Technical University of Athens (NTUA). As Fig. 3 illustrates, the site is a refurbished two-storey industrial site with a total surface area of approximately 534 m^2, with a total air volume of 2475.93 m^3.

Besides certain micro-climates in Greece, most of the country holds a Mediterranean climate. Lavrion is no exception, the weather around the test site is mostly sunny and dry during the summer, with precipitations in the form of showers or thunderstorms and mild winters with a surplus in rain and rarely any long lasting snow. Köppen Climate Classification characterizes the location of the test site is as a Hot-Summer Mediterranean Climate (Csa), commonly labeled as "typical Mediterranean climate" given that it is the most common form of sub-type Mediterranean climate. Statistically speaking it's coldest month averages above −3 to 0 °C, with at least one month's average temperature reaching above 22 °C, and at least four months temperature averaging above 10 °C. With winter's wettest month producing at least three times as much precipitation as the driest month of summer [53].

3.1. Building detail information

As mention before, this is a two-storey building, the architectural layout of the different thermal zones established is displayed in Fig. 4, where the ground floor holds: a kitchen, toilets, control/server room, the main entrance area, an atrium (hall), and an adjacent unconditioned storage area. The upper floor also hosts two offices, a meeting room and transit spaces.

Its envelope construction consists of double concrete block walls with single-glazed windows installed on aluminum frames. Additionally, it's external masonry consists of double brick wall's with 10 cm expanded polystyrene (EPS) insulation (U value = 0.25 W/m^2 K). The roof consists of metallic panels with a 2.5 cm polyurethane insulation layer in the middle (U value = 0.75 W/m^2 K).[54]

It is to be noted that H2SusBuild uses two separate HVAC systems deployed in parallel and that service completely different areas of the building, VRF system and a Heat Pump (HP) system. Since the scope of this study is to focus on the VRF system, the indoor spaces listed on Table 3 belong to main conditioned rooms that hold at least one VRF terminal unit equipment installed inside them, and therefore will be involved in the calibration process.

As for the remaining volumes of the building, 420.33 m^3 belong to unconditioned spaces such as storage areas, and the remaining 1114.62 m^3, belonging to the atrium, are conditioned through the independent HP system. These areas are modelled and their indoor behaviour is fixed to the input data obtained from the building temperature sensors, reducing any uncertainty from the adjacent areas by introducing into the simulation environment the effects of adjacent thermal zone's indoor temperatures.

As explained on Section 2, , to minimize the uncertainty produced by the envelope system, the following HVAC system has been introduced into a baseline BEM whose envelope is already calibrated using the methodology stated by Ramos et. al. [27], and validated by Gutiérrez et. al. [44].

3.2. HVAC system considerations

The sizing, design and commissioning of the building's installed HVAC equipment was a direct answer to the site weather constrains, in the form of a statistical weather data file that "recollects" the events from at least 30 years, and it's estimated indoor loads. This expected building's demand is what guides the design of any equipment installed in a building, just as there is a difference between expectation and reality, there is a gap between design and operation performance.

As stated at the beginning of Section 3 the test site is located in a "typical Mediterranean weather", which is characterised as a hot summer location with mild winters. This means the installed equipment in H2SusBuild is primarily focused on meeting the cooling demand produced by hot summer scenarios and may suggest that the same equipment could be oversized or have an important design gap when meeting the heating demand produced by mild winters. Forcing the system to operate on a completely different performance range during winter conditions and not on the range of it's nominal design conditions.

H2Susbuild main HVAC system which is subject to the current study, is a two-way pipe multi-split variable refrigerant flow

Fig. 3. Overview of H2Sus Test Site. On the left, a photograph of the test site main entrance. On the right, the overview of the generated BEM's geometry.

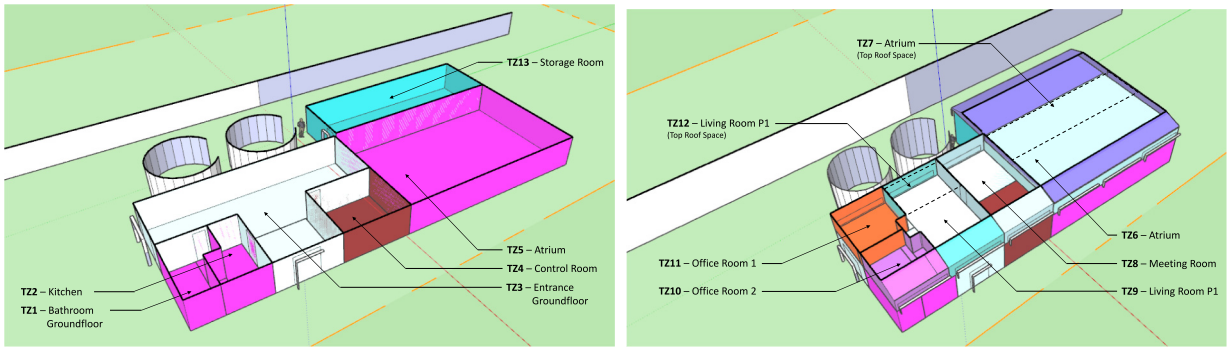

Fig. 4. H2Sus Test Site model displaying it's different thermal zones. Left, Ground Floor Plan. Right, First Floor Plan.

Table 3
Building conditioned thermal zone's effective floor area and indoor air volume.

	TZ02	*TZ03*	*TZ04*	*TZ08*	*TZ09*	*TZ10*	*TZ11*	*TOTAL*
Area (m^2)	13.72	98.39	25.38	50.43	54.44	23.85	23.82	290.03
Volume (m^3)	42.52	305.00	78.66	182.27	160.50	58.39	113.64	940.98

(VRF) system. Which is basically a direct expansion (gas-liquid) system whose rate of refrigerant flow varies by the operation of a variable speed compressor and multiple Electronic Expansion Valves (EEV) located in each indoor unit to match the thermal zone cooling or heating load in order to maintain the zone air temperature at a given set-point [1]. In other words, under this particular configuration, it can only provide either cooling or heating but not both at the same time. It is comprised of a tandem outdoor unit with a nominal cooling capacity of 71 kW (indoor temperature range: 15 to 24 °C; outdoor temperature range −5 to 43 °C) and a nominal heating capacity of 80 kW (indoor temperature range: 15 to 27 °C; outdoor temperature range −20 to 15.5 °C) connected to a total of 13 indoor wall mounted VRF fan-coil units (FCU) located in the different thermal zones across the building with the exception of the atrium.

As Fig. 5 describes, according to their nominal cooling and heating capacity, the wall mounted FCU instaled on H2Susbuild have been classified as: Type-28 (Cooling 2800W/ Heating 3200W), Type-45 (Cooling 4500W/ Heating 5000W), Type-56 (Cooling 5600W/ Heating 6300W), and Type-71 (Cooling 7100W/ Heating 8000W). Additionally, the tandem outdoor unit also provides heating and cooling to an auxiliary air handling unit used for ventilation by the means of a direct expansion coil whose nominal cooling capacity is 15 kW with a nominal heating capacity of 10 kW.

As for the second system, it serves exclusively to the building's atrium and outside the scope of this study. It is composed by an air handling unit interconnected to a water-to-air heat pump. To emulate it's effects inside the BEM, an ideal load system has been introduced in this section of the building's model set to match the simulated indoor climate of the atrium to it's real counterpart. This way we manage to introduce into the model the effects of any heat transference the atrium may have over nearby thermal zones while reducing the uncertainty originated from this system.

3.3. VRF simulation baseline BEM

The VRF scheme described on the previous section is modelled in detail in DesignBuilderV6 software, the model is then exported and introduced into EnergyPlus simulation environment. This process allows the application of multiple predefined components already located inside EnergyPlus simulation environment library, and the option of filling unknown parameter values of certain components with values belonging to similar equipment provided by DesignBuilderV6 database. It is here that HVAC units are interconnected to the building's thermal zones (TZ) nodes by a set of different components, loops, branches, pipes or ducts, describing the whole HVAC energy delivery scheme. Once this is performed, all known parameters values are set to the ones shown in the HVAC system's technical specifications and input data is loaded into the simulation environment for stressing purposes. The objective is to create a baseline model that describes the reality of the building and it's different systems as best as possible taking into account all the information available.

The interconnection and detailing of elements from H2susbuild's HVAC system is illustrated in Fig. 6, it is composed by two subsystems or "loops" working in parallel to condition the various indoor spaces of the building. The main subsystem is called "Variable Refrigerant Flow Loop" and is composed by an outdoor air conditioning (AC) unit connected to the different FCU mounted inside the building. On the other hand, the "Auxiliary Air Loop" whose purpose is provide ventilation into the spaces, is composed by an air handling unit with an air-to-air heat recovery system and direct expansion (DX) coils. In the figure, the round icons labeled as "T" stand for indoor temperature sensors deployed in each one of the different TZ, while the ones labeled with the letter "E" stand for equipment nodes in the simulation environment where the results for electric energy consumption will be obtained.

3.3.1. Variable refrigerant flow loop

Fig. 6 displays the building's spaces classified into three main groups depending on the number of actual fan coil units mounted inside them: one, two or four individual units. After this is performed the FCU are modelled inside each one of the TZ groups and their parameters are set to technical specification values. At this point, it is important to note that the units have been classified in four typical FCU based on the nominal cooling capacity of the installed equipment. The main reason behind this choice is to address the challenge regarding simulation run-time execution and computer processing power. [55] By grouping the FCU we reduce the search space of the calibration process, since having the parameters for all terminal units as optimization variables will end in an unmanageable large search space, this classification is a

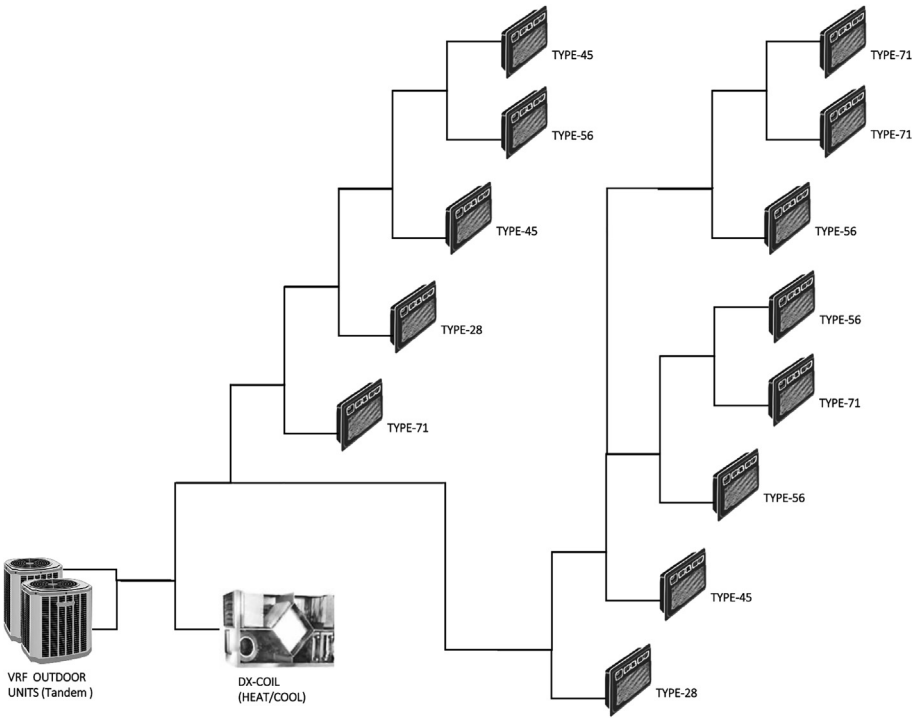

Fig. 5. Overview of H2Sus HVAC VRF Installation diagram.

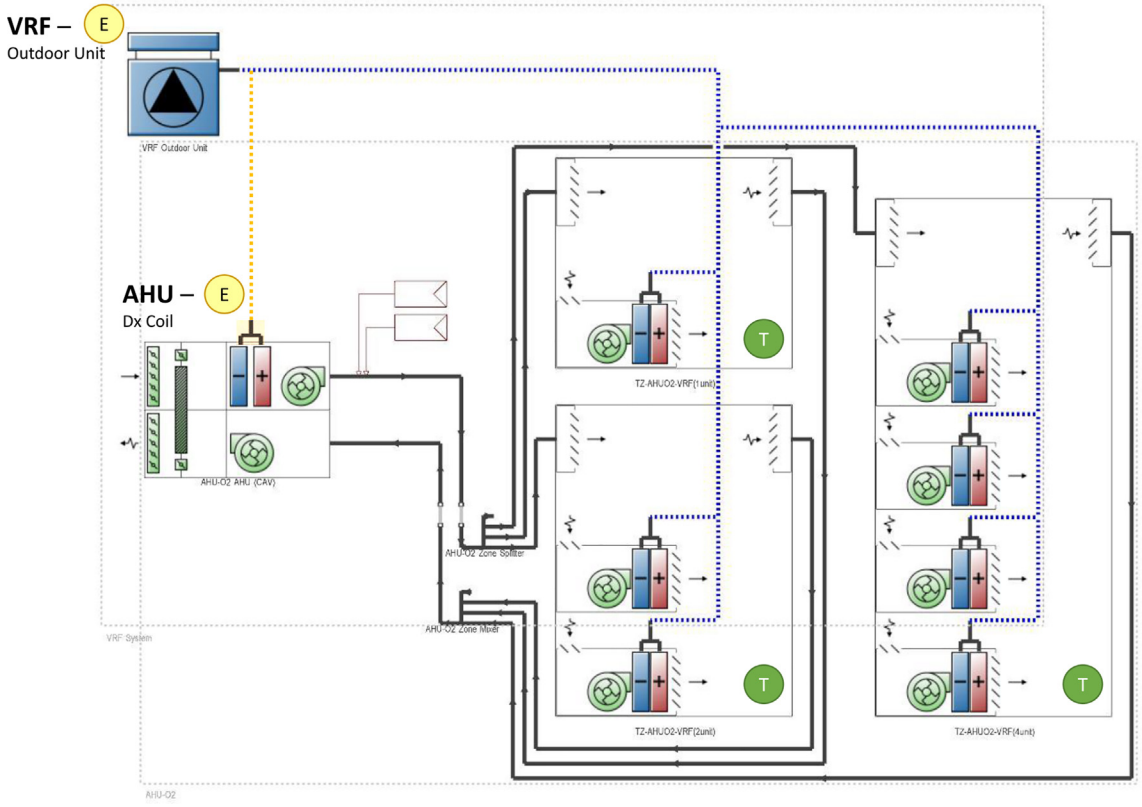

Fig. 6. Overview of H2Sus HVAC simulation environment.

necessary step even if it may seem we sacrifice some accuracy for calculation time.

The zone terminal FCU introduced in EnergyPlus simulation environment are a packet element composed by: either a draw through or blow through fan, an optional outside air mixer object that is turned off in the case of H2Susbuild, and a couple of direct expansion (DX) coils for heating and cooling that are used exclusively in conjunction with a variable refrigerant flow (VRF) air con-

ditioning (AC) system. The operation of each DX coil, be it cooling and/or heating, is specified depending on the operating mode required by the AC system. In relation to its performance, EnergyPlus states "The terminal units operate to satisfy a heating or cooling load in a zone based on a zone thermostat temperature set point." [56].

This is the reason why on this kind of systems there is a strong relationship between indoor climate, outdoor temperatures and the equipment electric consumption. This relationship is defined by the multiple performance curves of the DX coils and the AC system which are usually obtained from the equipment's technical documents. As Hydeman et. al. suggests these curves can be defined inside EnergyPlus simulation environment by executing a least-squares linear regression model to characterize them. [37,38] A process that results in the determination of the parameters labeled C_i shown in Eqs. 6 and 7, which define the mathematical shape and dimensions of a given curve aiming for them to resemble as close as possible to the ones that are set in the technical documents.

$$z = C_1 + C_2 * y + C_3 * y^2 + C_4 * y^3, \tag{6}$$

$$z = C_1 + C_2 * x + C_3 * x^2 + C_4 * y + C_5 * y^2 + C_6 * x * y, \tag{7}$$

where:

z = either cooling/heating capacity or electric consumption performance.

x = indoor air temperature (°C – wetbulb for cooling / drybulb for heating)

y = outdoor air temperature (°C – drybulb for cooling / wetbulb for heating)

C_i = coefficients that define the equation.

Depending on the component EnergyPlus may allow different kind of expressions to define this curves, this allows to establish different relationships between performance parameters depending on the information available. For example Eq. 6 usually links performance to one parameter, outdoor air temperature; while Eq. 7 shows a bi-quadratic expression that establishes a relationship between the equipment performance, indoor climate and outdoor temperatures.

In a way, the VRF system deployed functions like a thermal-electric transformer, it is constrain by the building indoor climate and by the application of these various performance curves we obtain the simulated electric consumption required to maintain the building's conditions under the site weather. Since the physical point for measure the equipment's electric consumption is the outdoor tandem unit and includes the effects of any sub components like fans as a whole, the curves defining the AC system and the indoor terminal fan coil units DX coils in terms of heating/cooling capacity and electric consumption are enough to describe the system behavior.

3.3.2. VRF component modelling

As such, the terminal FCU units installed inside the building's thermal zones have been grouped into four Type units: VRF-28, 45, 56, and 71 based on their nominal capacity as stated on Section 3.2. This four type units are introduced into the different TZ of the BEM their location based on the AC installation blueprints and the component performance parameters are set to the nominal values obtained from the HVAC system technical documents. Since there was no information regarding the performance curves of the DX cooling and heating coil placed inside the indoor FCU in the building's HVAC technical specification package, of the curves deployed in the modelled units where obtained from DesignBuilderV6 database. This includes the capacity ratio modifier function of temperature curve and, capacity modifier curve function of flow fraction as displayed on Fig. 7and8.

Since the overall performance of a VRF system is correlated to the location and interconnection of its FCU to the outdoor VRF unit, EnergyPlus allows the introduction of length and height performance correction factors in the VRF outdoor unit. These factors correct the VRF system performance by establishing the distance and height between the outdoor unit and the farthest connected FCU. As Fig. 9 displays, for both: cooling and heating operation modes, a piping correction factor function of length curve is defined inside EnergyPlus environment, ensuring that the generated BEM model that will be calibrated takes into account piping length factors.

The assessment of HVAC blueprints allows to measure the distance from the outdoor unit to the farthest FCU installed on the building. This distance is transformed into an equivalent length value aiming to represent fitting losses, pipe bends, and other connection factors present for both horizontal and vertical distances. Using the equation given by the equipment technical specification for equivalent length, Equation 8, an value of 34.71 m is obtained for this particular VRF system.

$$Equivalent\ L = Actual\ Piping\ Length + (0.7 \times N^{\circ}\ of\ Piping\ Bents), \tag{8}$$

As for the maximum height the FCU are installed, blueprints show a maximum difference of +3.90 m between the second floor FCU and the outdoor VRF unit installed on the ground floor level, establishing a height correction factor of $-0.0006\ ^1/m$ for both cooling and heating operation modes according to technical documentation.

To describe the outdoor unit multiple curves are required. Based on technical specifications for the installed equipment, all of the baseline parameters values are set and the following performance curves for cooling and heating operation modes are defined inside EnergyPlus simulation environment:

- Capacity Ratio Boundary Curve.
- Capacity Ratio Modifier Function of Low Temperature Curve
- Capacity Ratio Modifier Function of High Temperature Curve
- Energy Input Ratio Boundary Curve.
- Energy Input Ratio Modifier Function of Low Temperature Curve
- Energy Input Ratio Modifier Function of High Temperature Curve
- Energy Input Ratio Modifier Function of Low Part-Load Ratio Curve

While the following curves are set based on DesignBuilderV6 component library since there is no information available from the building's HVAC technical specifications.

- Energy Input Ratio Modifier Function of High Part-Load Ratio Curve
- Combination Ratio Correction Factor Curve
- Part-Load Fraction Correlation Curve

EnergyPlus VRF outdoor unit allows the use of both: a single set of curves that define the equipment's cooling or heating capacity and it's respective electric input disregarding outdoor temperature range, or a set of specific curves for Low and High outdoor temperature ranges. In which case, it is required to set boundary curves that define the limit between this Low and High temperature range. Fig. 10 shows the boundary curves applied for cooling and heating VRF operation mode used the BEM when required.

Fig. 11 describes the curve for energy input ratio modifier function of Low Part-Load Ratio (PLR) established with the information

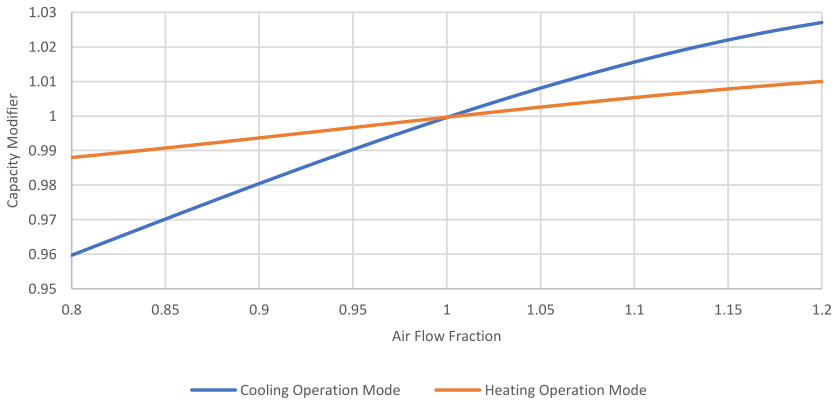

Fig. 7. Fan Coil Unit DX Coil capacity modifier curve function of flow fraction for Cooling and Heating operation generated for the BEM.

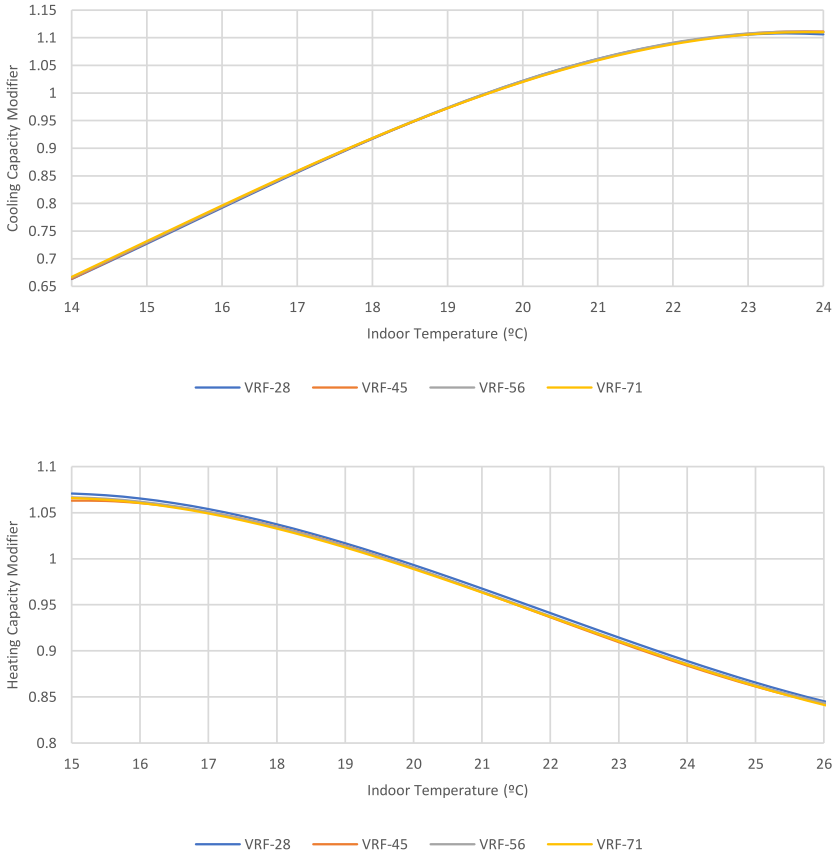

Fig. 8. Fan Coil Unit DX Coil capacity modifier curves function of indoor temperature for Cooling (above) and Heating (below) generated for the BEM.

from the equipment's technical specifications. This curve modifies the energy input ratio based on the PLR when it is less that 100%. In contrast, there was no information from the technical specification regarding the curve that describes the equipment working under a High PLR, that is when the PLR is above 100%. This particular set of curves was based on an equipment of similar characteristics found in DesignBuilderV6 library.

The same can be stated for the cooling combination ratio correction factor curve displayed on the left of Fig. 12, which describes the total rated indoor terminal unit cooling or heating capacity divided by the outdoor unit's respective rated total capacity. And the cooling part-load fraction correlation curve on the right of Fig. 12, which is used to define the cycling losses when the condenser's compressors cycle on and off. There was

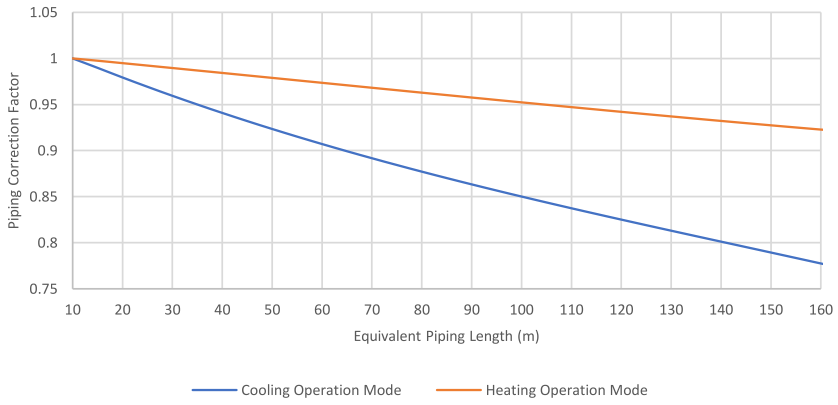

Fig. 9. Piping Correction Factor function of Length Curve for Cooling and Heating operation generated for the BEM.

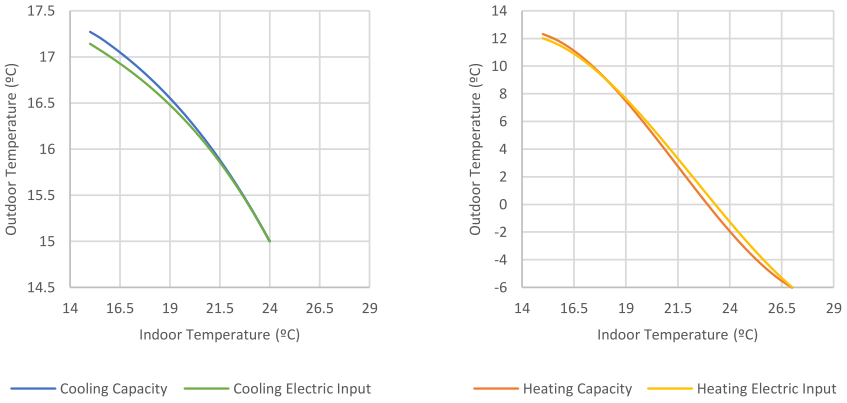

Fig. 10. Capacity and Electric Input Boundary Curves applied for Cooling (left) and Heating (right) operation mode used by the BEM.

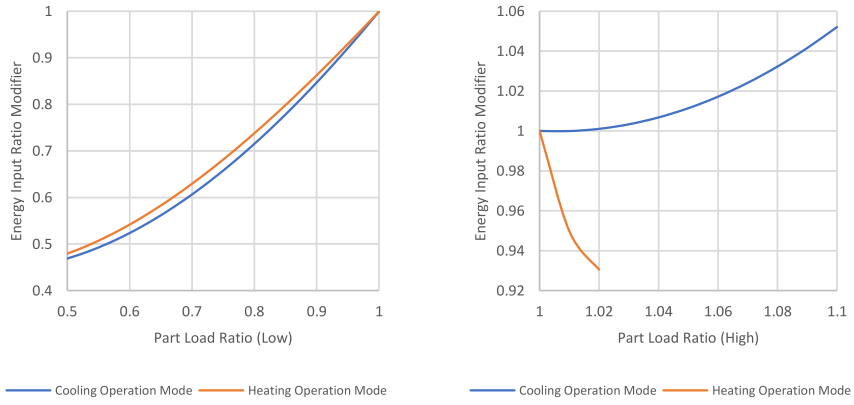

Fig. 11. Energy Input Modifier Curves for Cooling and Heating function of the Low Part Load Ratio (left) and High Part Load Ratio (right) used by the BEM.

no available information from the equipment's specifications, therefore both were introduced into the BEM from on an equipment of similar characteristics found in DesignBuilderV6 library.

It is clear that describing the behaviour of a VRF system requires multiple curves that work in conjunction with each other. In order to keep the solution search space on a manageable size, improve the run-time of the optimization process and reduce computational resources, this study assumes some of this curve's coefficient values as fixed. The current paper focus on the main curves that are key on describing the VRF behavior and that correlate indoor and outdoor conditions with the performance and electric input of the equipment. These curves are: Capacity Ratio Modifier Function of Low Temperature Curve, Capacity Ratio Modifier Function of High Temperature Curve, Energy Input Ratio Modifier Function of

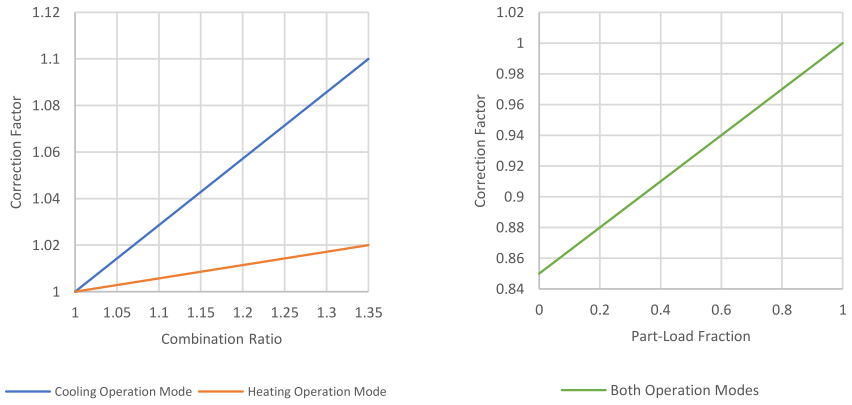

Fig. 12. Combination Ratio Correction Curves for Cooling and Heating (left) and Part Load Fraction Correction Factor Curve (right) used by the BEM.

Low Temperature Curve, and Energy Input Ratio Modifier Function of High Temperature Curve for both cooling and heating operational modes; displayed on Section 4.

3.3.3. Auxiliary air loop

The main purpose of this loop is to provide ventilation into the different building spaces. To do so, an Air Handling Unit (AHU) is connected to each one of the thermal zones by the use of an uncontrolled single duct air terminal unit. And a set-point manager is introduced in the air loop in order to control the supply air temperature for heating and cooling inside the spaces.

This auxiliary system is composed of an Air Handling Unit (AHU) connected to an air loop that provides ventilation into the same TZ of the main system. As defined in ANSI/AHRI Standard 430-2009 [57] an AHU is a factory made encased assembly package, this means inside of the equipment there are multiple components or subsystems to provide: filtration, heating, cooling, heat recovery, humidifying, dehumidifying and mixing of air. Inside EnergyPlus simulation environment the AHU element is quite similar in this regard as it holds inside multiple components that simulate it's real counterparts.

The AHU displayed in Fig. 6 contains two constant speed fan components, one for air supply and another for extraction, connected to an outdoor air system that does not recirculate air and includes a fixed-plate air-to-air heat recovery system. The AHU has two direct expansion (DX) coils (heating and cooling) modelled to represent the operation of the actual direct expansion element installed inside the equipment. [56] Since in reality this DX coil is connected to the outdoor AC unit, as the dotted yellow line indicates, the energy consumption obtained from the simulated DX coils will be sum to the one obtained from the outdoor VRF unit.

3.4. Data recollection and quality analysis

Section 2 details an inverse data driven process where both quality and quantity of available data influence the results of the quality of the calibration. As mention by the authors on their previous work [43], it is possible to categorize the data based on quality classification structures developed by the studies of Yang and Becerik-Gerber [23], Zhou and Park [58], Pan et. al. [59] and, Coackley et. al. [60], in order to prioritize it's use inside the simulation environment. Ranking information obtained from measurement as the best source for data, followed by survey data, operation manuals and building documents, manufacturer technical specifications, codes and standards, until least quality data of experience assumed values. The application of this structure allows to develop a BEM that inclused only data of the highest quality available.

In the case of H2Susbuild, a continuous monitorization campaign was launched through the summer of 2019 to the end of summer of 2020. It's objective, to collect fifteen minute time-step data stream from multiple sensors deployed inside the building, as well as, from the Building Management System (BMS) listed on Table 1. An activity executed with the help of an online data broker. When handling data obtained from an active physical location as it is the case of H2susbuild, the resulting data stream may contain errors or unforeseen faults from sensors and equipment alike, therefore an exhaustive analysis of the quality and quantity of the incoming data stream is performed. This process begins by filtering any missing or blank values. In the case of this study a specific rule flags any data gap greater than 3 hours discarding it from the calibration process; if the gap is under this threshold, the missing values are filled by applying a linear interpolation between two known values.

This continuous stream can now be cross checked in order to study the building's behaviour and it's HVAC system operation, a difficult task that aims to find unseen correlations and understanding the different subsystems [61]. For instance, the data collected from sensors and the Building Management System (BMS) regarding power rates can be cross-checked with indoor temperature allowing us to establish different equipment and components availability status. This analysis and comparison of data results in further clearing the stream from any sensor suspicious behaviour or equipment malfunctions, flagging these events for further examination and discarding the data from the calibration process. For example, a temperature sensor whose measured temperature seems fixed on a single value for over 3 hours to a full day is a clear example of a suspicious behaviour, the event is flagged, the stream cleaned from it's influence and the calibration continues; meanwhile, further inspection is performed on the building to establish if it is a problem with the sensor or the system and implement a solution.

The result of this process was a total of 4596 hours of valid operational data for this study, that is 2519 hours of valid operation in the lapse of one whole year, that means that for this study only 28.76% of hours in the year were deemed as viable. Divided into: 1717 hours (May to October 2019) for the summer calibration period, just 802 hours (November 2019 to April 2020) to perform the winter calibration process, and 2077 hours (May to August 2020) as checking period for the summer calibration results. The obtained data stream clearly signals how difficult it is to obtain one year of data for HVAC calibration purposes, even more when

there is a significant difference between operational behaviour between summer and winter conditions in the building's systems as Section 4.3 demonstrates. It is to be noted that the calibration process is performed on a fifteen minute time-step run, as it has been observed that keeping all data files to the same time-step size improves the simulation run-time.

3.4.1. Weather data

Weather is one of the main actors in building energy modelling [62]. This is because it stresses the building and directly influences it's energy demand to reach comfort indoor conditions, moreover weather affects the performance of the building's installed HVAC equipment [63,64]. This becomes evident when handling VRF systems, where for most cases cooling/heating performance and electric consumption curves are correlated directly to weather parameters. For this reason H2susbuild has a weather station that continuously monitors the conditions of the test site, delivering data to the broker on a fifteen minute time-step. Table 4 lists the weather station sensors deployed for this study and their accuracy.

3.4.2. Control data

As explained on Section 2, there are two key sets of data whose purpose is to benchmark the results obtained from the calibrated model. The measured electric consumption from the outdoor AC unit is compared against the simulated results from the BEM VRF electric consumption on an hourly basis using the previously mentioned ASHRAE Guidelines 14 [17] and IMPVP [16] standards. In the same fashion, we use CIBSE TM-63 [49] and VDI-6020:2002 [51] to help us validate if indoor temperature is maintained through the different spaces, by performing this multi-level benchmark we are also establishing how the consumed energy has been distributed, or delivered, across the different simulated building spaces.

4. Analysis of results and discussions

4.1. Summer calibration period

The established summer calibration period runs from May 2019 to October 2019, the weather details for this period can be seen on Table 5. The test site has a monthly average temperature of 24.5 °C that ranges from 19.5 to 28.1 °C, with relatively stable maximum temperatures that range from 30.6 to 36.6 °C being the months of July and August the hottest. While, May and October are the coolest with a monthly average minimum for the entire calibration period that ranges from 10.0 to 20.4 °C.

Section 3.2 mentions that H2susbuild HVAC system is a two-way pipe VRF, this means that during summer both: the outdoor AC unit and all indoor FCU settings are locked to provide cooling only into the building. If by any reason the building's indoor spaces demands heating, the system providing cooling shuts down. This simple operation fact is important to understand the HVAC system and establish its behaviour, specially once we take the weather into account.

As stated in Section 3.3.1, the FCU have been classified into four groups by their nominal cooling capacity. Table 6 displays the parameter values for the indoor FCU obtained after the calibration process had ended. It is to be noted that except for VRF-45 and VRF-56, under this summer scenario the values for nominal cooling power of the FCU do not vary; and when they do, they barely do so.

In a similar fashion, the calibrated value for the outdoor AC unit nominal cooling power is 69.2 kW, as displayed in Table 7, is close to its nominal value of 71 kW. Furthermore, the obtained calibrated value for the Coefficient of Performance (COP) of this element is 3.2, 27.3% lower than its nominal value of 4.4 but still seems within a reasonable range. When we study this results as a whole, taking into account the resulting performance curves for the AC VRF outdoor unit and the parameter values obtained for both the indoor FCU and the VRF outdoor unit, this apparent loss in efficiency may actually signal normal equipment deterioration due to it's lifetime running hours.

When analysing the results obtained for the curves introduced in the AC VRF outdoor unit, we must first consider the following. There are multiple ways to approach the calibration process of a system like this one, if we where to fix the curves values to technical specification and optimize the rest of the equipment's parameters we are finding the best solution of parameter values for a given performance curve set. However if we do the inverse, and fix all parameters to technical specification only to optimize the performance curve values, we are seeking for the best curve for this parameter set. When we aim to seek for both at the same time: curve coefficients and equipment values, we aim to obtain the best group or "family" of solutions for the system. Once this is achieved one could, if needed, use any of the previously described approaches to close further into a solution knowing it will be the "best" for a given constrain condition (curve or parameter value).

The performance curves for cooling capacity and electric consumption obtained from technical specifications allowed their introduction into EnergyPlus simulation environment using a simplified calculation approach, where the simulated VRF outdoor unit will work only with one set of curves for both "Low" and "High" outdoor temperature conditions. This curve served as the base to step into a more complete model, where we set forth to seek these two different set of curves with the objective to better define the behaviour of the unit under different "Low" and "High" outdoor temperature ranges.

In terms of cooling capacity, Fig. 13 shows there is little difference between the shape, and amplitude of using these two set of curves in comparison with the original curve. Yet, in terms of electric consumption, the shape of the curves may be similar, but the amplitude has changed. This change is more evident with the High temperature range curve than the one obtained for the Low temperature one, and as we will see on Table 9, using these Low/High

Table 4
Weather station sensors and accuracy's values for H2SUS, Lavrion – Greece Test Site.

Sensor	Units	Range	Resolution	Accuracy
Temperature	°C	−40° to +65°	±0.1	±0.5
Humidity	%	0 to 100	±1.0	±3.0% (0–90) ±4.0% (90–100)
Global Solar Radiation	W/m^2	0 to 1500	1	≤10
Diffuse Solar Radiation	W/m^2	0 to 1500	1	≤20
Wind Speed	m/s	1 to 67	0.44	±1/±5%
Wind Direction	°	1 to 360	1.0	±4%
Precipitation	mm	–	0.2	±4%/0.25 (⩽50 mm) ±5%/0.25 (⩾50 mm)
Atmospheric Pressure	mbar	880 to 1080	±0.1	±1

Table 5
On-Site Summer training period weather details from May 2019 to October 2019. Table shows hourly maximum, average and minimum Outdoor DryBulb Temperature, average Global and Diffuse Radiation.

Description		Units	Training Period 2019						
			May	Jun	Jul	Aug	Sep	Oct	Average
			COOLING						
Outdoor DryBulb Temperature	Average	°C	19.536	26.208	27.545	28.185	24.243	21.137	24.476
	Maximum	°C	30.600	34.400	36.600	35.900	30.800	29.400	32.950
	Minimum	°C	10.000	16.600	19.100	20.400	14.400	13.700	15.700
Global Horizontal Radiation	Average	W/m^2	430.879	488.231	490.833	490.507	424.419	326.207	441.846
Diffuse Radiation	Average	W/m^2	285.090	305.600	294.535	285.452	216.690	141.005	254.729

Table 6
Comparison of parameter values between the Baseline BEM and Calibrated BEM obtained after the calibration process of the VRF Indoor FCU located inside the building Thermal Zones for the Summer Training Period 2019.

Equip.	Component	Parameter	Units	Baseline Model	Calibrated Model
VRF-28	DX Cooling Coil	Gross Rated Total Cooling Capacity	W	2800	2800
		Gross Rated Sensible Heat Ratio	–	autosize	0.75
		Rated Air Flow Rate	m^3/s	0.108300	0.113715
VRF-45	DX Cooling Coil	Gross Rated Total Cooling Capacity	W	4500	4600
		Gross Rated Sensible Heat Ratio	–	autosize	0.75
		Rated Air Flow Rate	m^3/s	0.183300	0.142058
VRF-56	DX Cooling Coil	Gross Rated Total Cooling Capacity	W	5600	5500
		Gross Rated Sensible Heat Ratio	–	autosize	0.75
		Rated Air Flow Rate	m^3/s	0.233300	0.204138
VRF-71	DX Cooling Coil	Gross Rated Total Cooling Capacity	W	7100	7100
		Gross Rated Sensible Heat Ratio	–	autosize	0.75
		Rated Air Flow Rate	m^3/s	0.258300	0.193725

Table 7
Comparison of parameter values between the Baseline BEM and the Calibrated BEM after the calibration process of the VRF Outdoor Unit took place for the Summer Training Period 2019.

VRF Outdoor Unit Parameter	Units	Baseline Model	Calibrated Model	
Gross Rated Total Cooling Capacity	W	71000	69225	
Gross Rated Cooling COP	W/W	4.4	3.2	
Cooling Capacity Ratio Modifier Function of Temperature Curve Name			Low	High
Coefficient C1	–	0.4519455	0.5300720	0.5738673
Coefficient C2	–	0.0312906	0.0240624	0.0308511
Coefficient C3	–	0.0002693	0.0004201	0.0003016
Coefficient C4	–	0.0050749	0.0000249	−0.0030717
Coefficient C5	–	−0.0001336	−0.0000003	0.0000039
Coefficient C6	–	−0.0002292	−0.0000013	−0.0002568
Minimum Value of x	°C	15.000	15.000	15.000
Maximum Value of x	°C	24.000	24.000	24.000
Minimum Value of y	°C	−5.000	−5.000	15.000
Maximum Value of y	°C	43.000	17.272	40.000
Cooling Energy Input Ratio Modifier Function of Temperature Curve Name			Low	High
Coefficient C1	–	−0.7736065	−1.3746840	−1.8260023
Coefficient C2	–	0.1314158	0.1897413	0.2194040
Coefficient C3	–	−0.0029907	−0.0043732	−0.0051608
Coefficient C4	–	0.0009882	0.0033681	0.0107644
Coefficient C5	–	0.0002172	−0.0000056	0.0000145
Coefficient C6	–	0.0000604	−0.0000001	0.0001933
Minimum Value of x	°C	15.000	15.000	15.000
Maximum Value of x	°C	24.000	24.000	24.000
Minimum Value of y	°C	−5.000	−5.000	15.000
Maximum Value of y	°C	43.000	17.143	40.000

curves work to better represent the consumption output of the simulated VRF outdoor unit.

The methodology was applied to the auxiliary air loop as well, the AHU unit has limited information about it's components and has forced us to make some assumptions on this system's components. We believe this to be positive for this study, since we are actually working under a scenario that closely resembles what happens most of the time in practice.

The air-to-air heat recovery sub-system parameters were calibrated in conjunction with the DX coil as this element is deployed inside the AHU prior to any other component and it's operation affects the performance of all of the equipment. The results shown

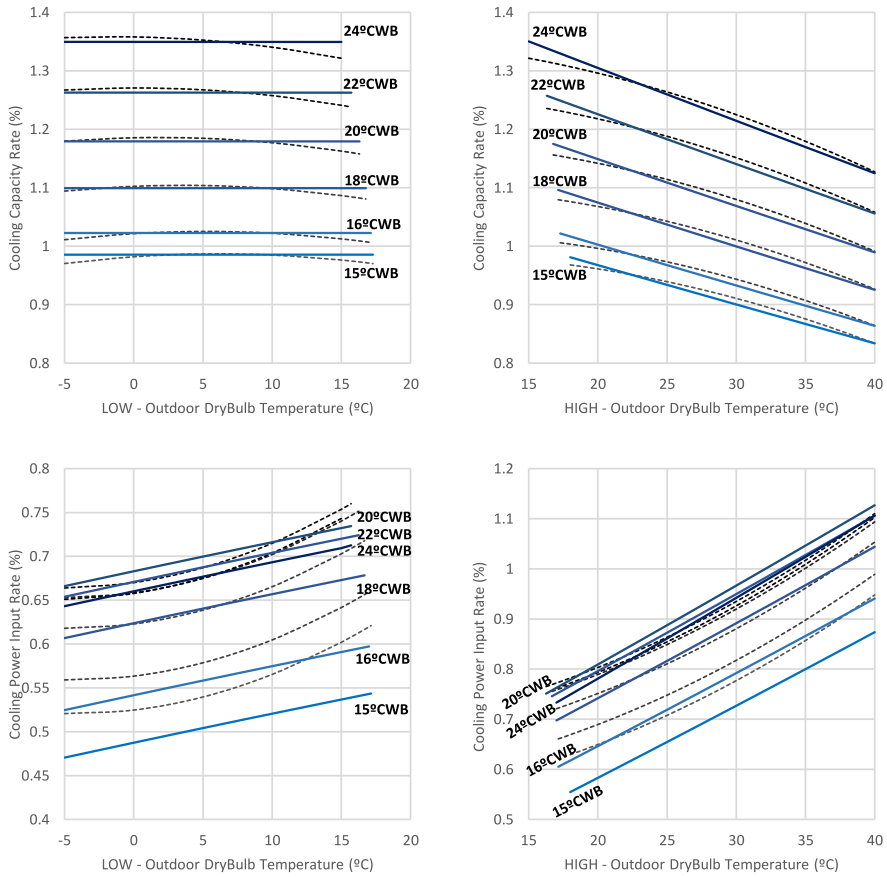

Fig. 13. VRV Cooling performance curves: Cooling Capacity for Low and High Outdoor temperature ranges (above) and Cooling Input for Low and High Outdoor temperature ranges (below) generated for the Baseline BEM (obtained from technical documentation) displayed in black and for the Calibrated BEM obtained after the optimization process displayed in blue. (For interpretation of the references to colour in this figure legend, the reader is referred to the web version of this article.)

Table 9
Electric Consumption hourly uncertainty index for the Cooling Calibration period using 1717 hours of operation between May 2019 to October 2019.

	International Standard		Electric Consumption Results	
INDEX	ASHRAE	IMPVP	Baseline Model	Calibrated Model
NMBE	±10%	±5%	−19.207%	7.139%
Cv(RMSE)	30%	20%	36.263%	25.681%
R^{2a}	75%	75%	57.289%	75.300%

[a]Although there is no universal standard for a minimum acceptable R^2 threshold, values above 75% are often considered a sign of a good causal relationship amongst the energy and independent variables.[16].

in Table 8 display a loss of effectiveness in all parameters, i.e. around 21% of sensible effectiveness loss at 100% rate (from 0.80 to 0.63). Which may signal either the design gap of the equipment performance, or it's natural loss due to operation run-time, or both.

Besides their nominal cooling/heating power and COP, the building's technical documents show no information available regarding the performance curves of the DX coil installed inside the AHU, it was decided to apply the same baseline curves obtained for the VRF outdoor unit, as Table 8 shows. The main difference between this element and the AC VRF outdoor unit relies in the calculation approach used to establish it's behaviour; in this particular case there is no "Low" or "High" outdoor temperature ranges, a single bi-quadratic curve is enough to define it's cooling capacity performance and power consumption performance.

As stated in Section 3.4.1 weather plays an important factor in VRF systems, more so when being constrained to use only one curve to define the behaviour of the coil regardless of any outdoor temperature range. In the case of cooling capacity, displayed on the left of Fig. 14, we see that the calibrated curve seems to fit the baseline model one when outdoor temperatures are above +10 °C. Something similar seems to occur on the electric input curve, yet in this case the curves invert when the outdoor temperatures are below the previously mentioned threshold. It would seem that under this DX "single" curve model, the coefficient values that result from the calibration process seem to have adapted so that the behavior of the equipment fits into the temperature range that is more common during the training period.

What we see after the calibration process has ended is an improvement in the behavior of the HVAC system electric consumption when compared to actual readings obtained from the building. Fig. 15 shows an improvement in capturing the electric consumption for the whole calibration period from a +19.21% to a −7.14% (NMBE). Moreover, in the dispersion graph in the figure shows how the calibration process rearranges the simulated

Table 8
Comparison of parameter values between the Baseline BEM and the Calibrated BEM after the calibration process of the Air Handling Unit and it's expansion coil for the Summer Training Period 2019.

Equip.	Component	Parameter	Units	Baseline Model	Calibrated Model
AHU	Air to Air	Nominal Supply Air Flow Rate	m^3/s	0.5555560	0.4200000
	Heat	Sensible Effectiveness at 100% Cooling Air Flow	–	0.80	0.63
	Exchanger	Latent Effectiveness at 100% Cooling Air Flow	–	0.71	0.65
		Sensible Effectiveness at 75% Cooling Air Flow	–	0.83	0.75
		Latent Effectiveness at 75% Cooling Air Flow	–	0.72	0.65
	Cooling	Gross Rated Total Cooling Capacity	W	15000	12000
	DX Coil	Gross Rated Sensible Heat Ratio	–	autosize	0.75
		Gross Rated Cooling COP	W/W	2.70	2.20
		Rated Air Flow Rate	m^3/s	0.6030000	0.9644440
	Cooling	Total Cooling Capacity Function of Temperature Curve Name			
	DX Coil	Coefficient C1	–	0.4519455	0.9425893
		Coefficient C2	–	0.0312906	0.0095434
		Coefficient C3	–	0.0002693	0.0006838
		Coefficient C4	–	0.0050749	−0.0110427
		Coefficient C5	–	−0.0001336	0.0000052
		Coefficient C6	–	−0.0002292	−0.0000097
	Cooling	Energy Input Ratio Function of Temperature Curve Name			
	DX Coil	Coefficient C1	–	−0.7736065	0.3423629
		Coefficient C2	–	0.1314158	0.0348798
		Coefficient C3	–	−0.0029907	−0.0006236
		Coefficient C4	–	0.0009882	0.0049765
		Coefficient C5	–	0.0002172	0.0004379
		Coefficient C6	–	0.0000604	−0.0007279

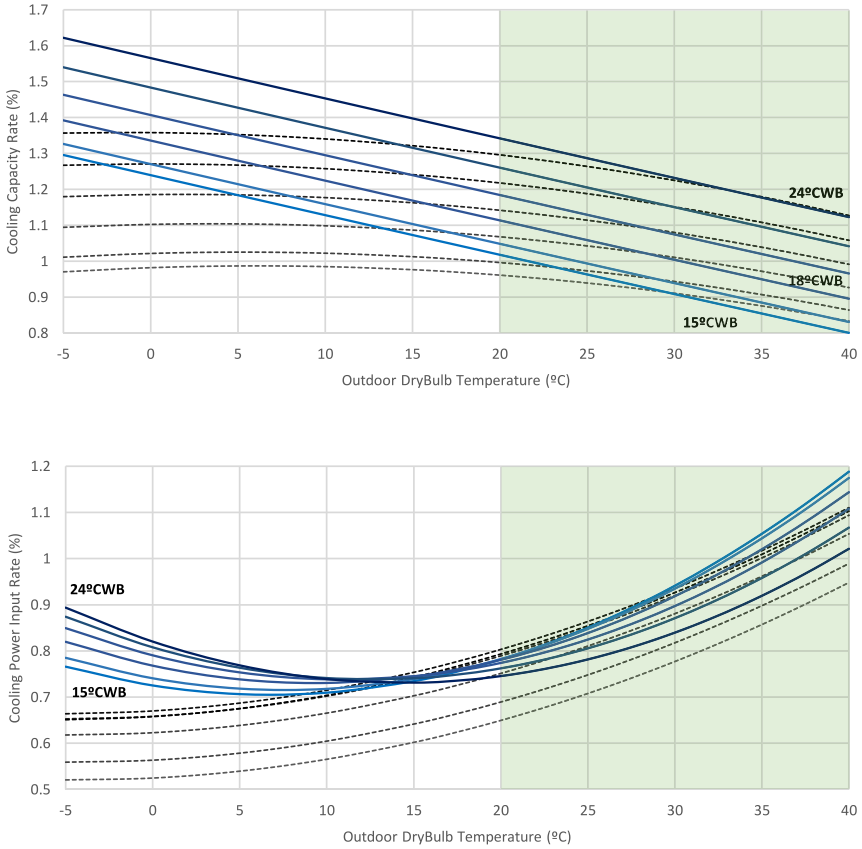

Fig. 14. Cooling Coil performance curves for the AHU DX Cooling Coil component: Cooling Capacity (above) and Heating Input (below) generated for the Baseline Model (obtained from DB technical library for a similar equipment) displayed in black and for the Calibrated Model obtained after the optimization process displayed in blue.

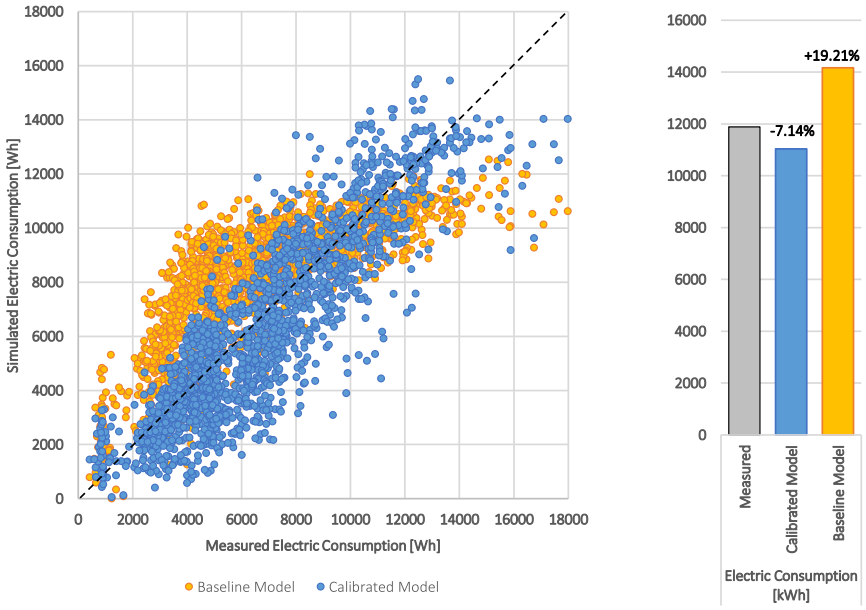

Fig. 15. Performance results for electric consumption of the calibrated BEM during the cooling calibration period from May 2019 to October 2019.

results for each hour, clustering them around the 45° line that stands for a theoretical perfect model.

As explained before, the quality of any BEM or it's fitting into real conditions can be measured through the indices exposed in Section 2.2. In the case of H2Susbuild, the calibrated BEM model results for the 2019 summer period are within the international limits set by ASHRAE for energy performance, reaching a Cv(RMSE) of 25.68% and complying with the standard recommendations of an R^2 above 75% as Table 9 shows.

And this is performed while maintaining indoor climate within the standards and recommendations of CIBSE TM-63 and the VDI-6020:2002, below a MAE of 2 °C and a RMSE of 1.5 °C for all the different thermal zones as displayed on Table 10. Which is a sign that the BEM is also distributing the energy correctly throughout the different thermal zones.

The previously exposed results, seems to indicate that the calibrated BEM with it's detailed HVAC system has captured the behaviour of the building and it's installed HVAC counterpart for the selected training period.

4.2. Summer checking period

An evaluation period is required to check the BEM model overall stability through time. Furthermore, stressing the calibrated BEM model with previously unseen data allows us to check if the process has over-fitted it's parameter values to the point they solely work with the training period data.

H2Susbuild checking period is displayed on Table 11 and comprises summer 2020 from May to August. The average monthly temperature for this period ranges from 20.1 °C to 27.9 °C. As with 2019, the months of July and August remain the hottest, this time with a maximum temperature 36.1 °C for the whole period and a minimum of 11 °C.

The results displayed on the dispersion graph in Fig. 16 shows that the calibrated BEM hourly electric consumption results keep clustering the 45° line in a rather uniform pattern. Regarding the residual for the whole checking period (NMBE) the calibrated model results seem stable through time, the simulated electric consumption differs from the measurement a 6.4% for this new period, close to the −7.14% previously obtained with the 2019 data.

In terms of Cv(RMSE) the results show that even though the BEM model remains within the threshold set by ASHRAE with 29.27% there is a loss of quality when comparing with the 25.68% obtained from the training period. It would seem this loss of quality is to be expected since the model is currently stressed with a new set of previously unseen data stream. Table 12

The two-level benchmark explained in Section 2 requires to check both energy consumption and indoor temperature. The energy consumption results are obtained while maintaining indoor climate conditions in all of the building TZ within international standards for MAE and RMSE as Table 13 shows, which suggest the energy is still being correctly distributed across the building. As with energy, when comparing the results of 2019 period in Table 10 with the ones of the checking period we see that there is a loss of quality due to the new stressing conditions, for instance

Table 10
Indoor thermal zone temperature hourly uncertainty index for the Cooling Calibration period using 1717 hours of operation between May 2019 to October 2019.

	Indoor Temperature by TZ							Building
INDEX	Tz-02	Tz-03	Tz-04	Tz-08	Tz-09	Tz-10	Tz-11	Average
MAE (°C)	0.235	0.054	0.024	0.057	0.138	0.221	0.328	0.100
RMSE (°C)	0.389	0.195	0.046	0.173	0.394	0.619	0.654	0.194
NMBE (%)	−0.584	0.000	−0.004	0.153	0.538	−0.410	−0.810	−0.014
Cv(RMSE) (%)	1.825	0.934	0.189	0.723	1.626	2.844	3.030	0.863
R^2 (%)	93.253	95.819	99.803	98.762	95.021	83.565	73.754	96.759

Table 11
Summer checking period weather details from May 2020 to August 2020. Table displays hourly maximum, average and minimum Outdoor DryBulb Temperature, average Global and Diffuse Radiation.

Description		Units	Training 2019	Checking / Evaluating Period 2020				
			Average	May	Jun	Jul	Aug	Average
				COOLING				
Outdoor DryBulb Temperature	Average	°C	24.476	20.086	24.403	27.619	27.905	25.003
	Maximum	°C	32.950	32.700	33.800	34.800	36.100	34.350
	Minimum	°C	15.700	11.000	14.800	18.800	19.800	16.100
Global Horizontal Radiation	Average	W/m^2	441.846	464.756	497.035	505.286	471.676	484.688
Diffuse Radiation	Average	W/m^2	254.729	349.252	325.661	273.185	281.664	307.440

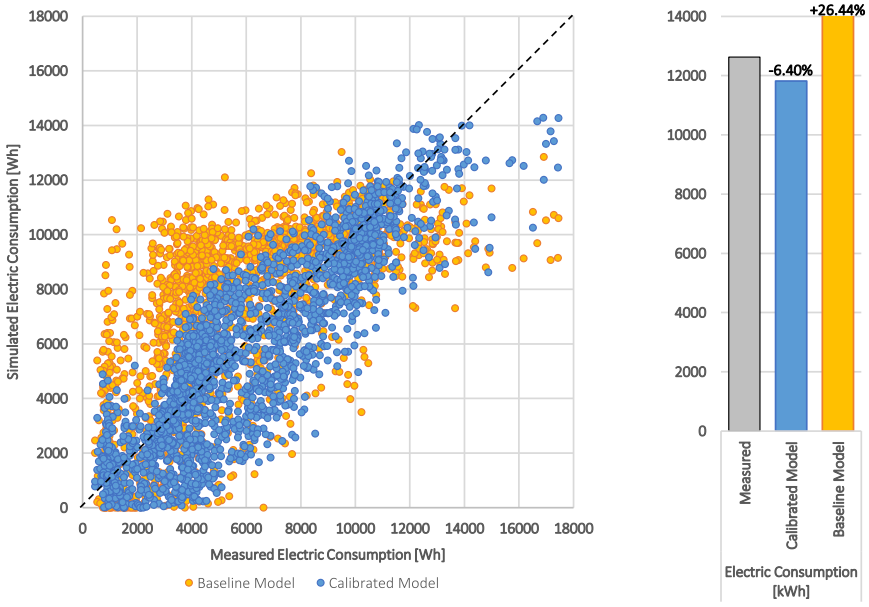

Fig. 16. Performance results for electric consumption of the calibrated BEM during the cooling checking period from May 2020 to August 2020.

Table 12
Electric Consumption hourly uncertainty index for the Cooling Checking period using 2077 hours of operation between May 2020 to August 2020.

	International Standard		Electric Consumption Results	
INDEX	ASHRAE	IMPVP	Baseline Model	Calibrated Model
NMBE	±10%	±5%	−26.442%	6.404%
Cv(RMSE)	30%	20%	53.747%	29.265%
R^{2a}	75%	75%	36.445%	75.237%

[a]Although there is no universal standard for a minimum acceptable R^2 threshold, values above 75% are often considered a sign of a good causal relationship amongst the energy and independent variables.[16].

Table 13
Indoor thermal zone temperature hourly uncertainty index for the Cooling Checking period using 2077 hours of operation between May 2020 to August 2020.

	Indoor Temperature by TZ							Building
INDEX	Tz-02	Tz-03	Tz-04	Tz-08	Tz-09	Tz-10	Tz-11	Average
MAE (°C)	0.303	0.082	0.051	0.100	0.193	0.218	0.308	0.135
RMSE (°C)	0.482	0.187	0.132	0.297	0.544	0.419	0.531	0.265
NMBE (%)	−0.407	0.214	0.135	0.359	0.773	0.155	0.125	0.297
Cv(RMSE) (%)	2.210	0.865	0.532	1.235	2.240	1.887	2.381	1.154
R^2 (%)	76.770	95.024	98.050	95.614	84.766	82.102	73.593	92.431

the building average RMSE is 0.265 °C, 36.6% higher than the 0.194 °C obtained during training.

Regarding the results of indoor temperature presented in Table 10 and Table 13 where the indices NMBE and Cv(RMSE) have been placed for comparison purposes only, it is obvious that using the threshold set for energy consumption by ASHARAE or IMPVP as a temperature index is wrong. If used, indoor temperature NMBE and Cv(RMSE) should have much more restrictive limits. For example, in the present study had a RMSE of 0.5°C is correlated to a Cv (RMSE) of around 2.2%, it could make sense that the limit for this index could be set around 7.5 to 5% for temperature benchmark, but further statistical analysis studies are required to set the exact limit value.

4.3. Winter training period

The present study only contemplates the use of one winter season, 2019-20, which holds only 802 hours of HVAC operational data throughout the whole six months the HVAC system is set for heating. For this reason all of the data collected was used for calibration/tranining purposes. Even if there is no winter checking period established for this study, we believe there are some important lessons that can be obtained from the winter calibration period. The results obtained from this study are an important part of the discussion and we feel the need to lay them out.

Since the HVAC system installed in H2Susbuild is a two-way pipe VRF set up, during the period from November 2019 to April 2020, the outdoor AC units are shifted and locked into heating mode. This corresponds to the winter training period 2019-20 where, as Table 14 shows, the average monthly temperatures range from 10.34 to 18.29 °C, with monthly minimum temperatures from 2.1 to 11.2 °C making January and February as the coldest months, and a maximum average temperatures for the whole period set at 22.33 °C. All signs of a typical Mediterranean climate with a mild winter season as previously exposed in Section 3.

In contrast with the results obtained during summer, Table 15 shows that under the winter scenario there is a drop of the gross rated heating capacity for all the terminal FCU's DX coil when compared to its nominal counterparts set in the baseline model. Being Type-71 the less affected with just a drop of 3.21%, while Type-56 falls a 14.77%, Type-45 a 12.02% and Type-28 a 12.03%.

As with the indoor FCU, the results for the AC VRF outdoor unit displayed in Table 16 show there is a reduction of it's rated heating capacity to 75.8 kW. And although it may seem that this reduction of just 5.25% is minor, the drop of 53.4% for the equipment's COP value reaching a mere 1.60 value is not. The obtained results suggest that the equipment is operating outside it's design range, or under conditions that are clearly penalizing it's efficiency.

This idea is further reinforced after analysing the curves obtained for the VRF outdoor unit. Since there is no manipulation of any part-load-ratio curve in this study, the behaviour of the equipment is solely described by the curves displayed in Fig. 17. In regards to the heating capacity curve, drawn on the left, after the calibration there is an uniform drop in efficiency of the equipment through the whole outdoor temperature range, this translates into a decrease of the unit's heating output as well. While in terms of heating power input curve, shown to the right, there is a difference between the equipment working on "Low" and "High" temperature range. We can see how both calibrated and baseline curves show that this VRF outdoor unit will operate under the better efficiency conditions on "Low" temperature ranges than at "High" temperature range. Moreover, we can see that with the rise of outdoor temperature the heating efficiency of this particular equipment greatly decreases.

Given the mild winter at Lavrio, which sets most temperatures during operational hours of the equipment on the border edge of the "High" operational range with a monthly mean of 13.74 °C and lowers the heating demand value inside the spaces. It is clear weather plays an important factor in establishing the performance of these VRF systems. The current conditions make the equipment

Table 14
Winter training period weather details from November 2019 to April 2020. Table displays hourly maximum, average and minimum Outdoor DryBulb Temperature, average Global and Diffuse Radiation by month, for the test site.

Description		Units	Training Period						
			2019		2020				
			Nov	Dec	Jan	Feb	Mar	Apr	Average
					HEATING				
Outdoor DryBulb Temperature	Average	°C	18.290	13.087	10.343	12.152	13.509	15.059	13.740
	Maximum	°C	26.900	19.800	18.500	20.300	23.800	24.700	22.333
	Minimum	°C	11.200	5.700	2.100	3.600	4.300	6.900	5.633
Global Horizontal Radiation	Average	W/m^2	216.122	149.558	181.237	281.833	357.178	435.048	270.163
Diffuse Radiation	Average	W/m^2	62.785	51.602	120.787	162.467	214.802	271.270	147.286

Table 15
Comparison of parameter values between the Baseline BEM and the Calibrated BEM after the calibration process of the VRF Indoor Terminal Units located inside the building Thermal Zones for the Winter Training period 2019–2020.

Equip.	Component	Parameter	Units	Baseline Model	Calibrated Model
TYPE-28	DX Heating Coil	Gross Rated Heating Capacity	W	3200	2815
		Rated Air Flow Rate	m^3/s	0.108300	0.101800
TYPE-45	DX Heating Coil	Gross Rated Heating Capacity	W	5000	4399
		Rated Air Flow Rate	m^3/s	0.183300	0.225907
TYPE-56	DX Heating Coil	Gross Rated Heating Capacity	W	6300	5369
		Rated Air Flow Rate	m^3/s	0.233300	0.226921
TYPE-71	DX Heating Coil	Gross Rated Heating Capacity	W	8000	7743
		Rated Air Flow Rate	m^3/s	0.258300	0.419988

Table 16
Comparison of parameter values between the Baseline BEM and the Calibrated BEM obtained after the calibration process of the VRF Outdoor Unit took place for the Winter Training Period 2019-2020.

VRF Outdoor Unit Parameter	Units	Baseline Model		Calibrated Model	
Gross Rated Heating Capacity	W	80000		75802	
Gross Rated Heating COP	W/W	3.43		1.60	
Cooling Capacity Ratio Modifier Function of Temperature Curve Name					
		Low	High	Low	High
Coefficient C1	–	0.8982883	1.5321780	0.6995828	1.3552587
Coefficient C2	–	0.0038412	−0.0204103	0.0031530	−0.0196267
Coefficient C3	–	−0.0002172	−0.0003492	−0.0001843	−0.0003317
Coefficient C4	–	0.0229511	0.0020792	0.0208050	0.0021216
Coefficient C5	–	0.0000074	−0.0000267	0.0000074	−0.0000260
Coefficient C6	–	−0.0001954	−0.0000642	−0.0001826	−0.0000664
Minimum Value of x	°C	15.000	15.000	15.000	15.000
Maximum Value of x	°C	27.000	27.000	27.000	27.000
Minimum Value of y	°C	−20.000	−6.020	−20.000	−6.020
Maximum Value of y	°C	12.316	15.000	12.316	15.000
Cooling Energy Input Ratio Modifier Function of Temperature Curve Name					
		Low	High	Low	High
Coefficient C1	–	0.6604075	3.0328816	0.5999514	2.4459882
Coefficient C2	–	0.0124444	−0.1047730	0.0119319	−0.0855209
Coefficient C3	–	0.0000742	0.0007861	0.0000709	0.0008394
Coefficient C4	–	0.0081086	−0.0993422	0.0069237	−0.1205840
Coefficient C5	–	0.0001907	0.0007285	0.0001792	0.0006432
Coefficient C6	–	0.0000761	0.0025502	0.0000615	0.0021472
Minimum Value of x	°C	15.000	15.000	15.000	15.000
Maximum Value of x	°C	27.000	27.000	27.000	27.000
Minimum Value of y	°C	−20.000	−5.991	−20.000	−5.991
Maximum Value of y	°C	12.014	15.000	12.014	15.000

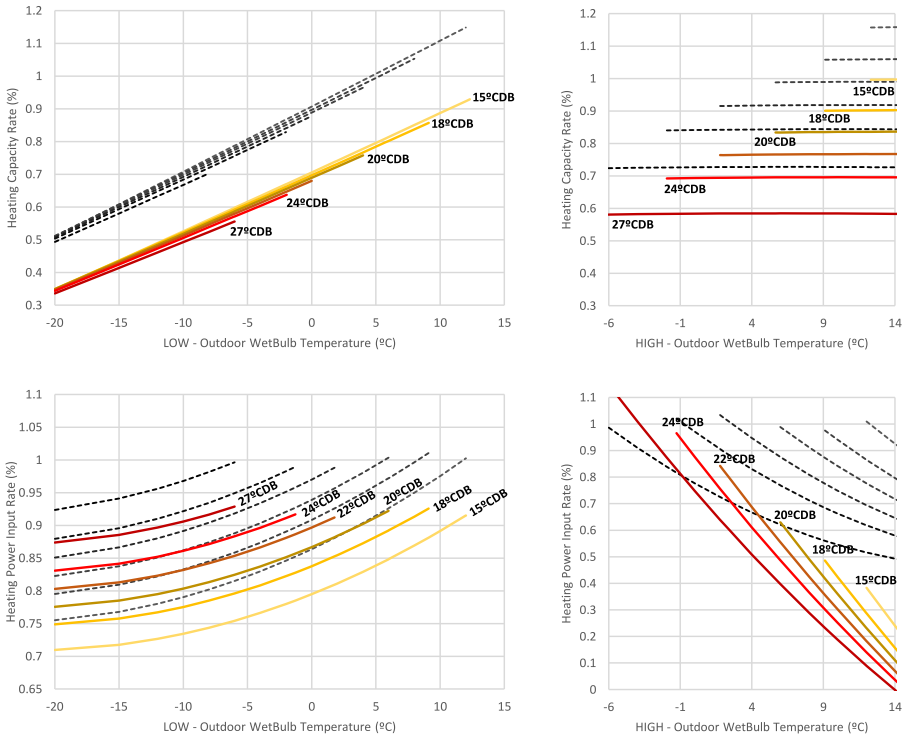

Fig. 17. VRV Heating performance curves: Heating Capacity for Low and High Outdoor temperature ranges (above) and Heating Input for Low and High Outdoor temperature ranges (below) generated for the Baseline BEM (obtained from technical documentation) displayed in black and for the Calibrated BEM obtained after the optimization process displayed in red. (For interpretation of the references to colour in this figure legend, the reader is referred to the web version of this article.)

work on an extremely low part load ratio, a performance zone where the EnergyPlus model has problems performing as intended according to Yun and Song [34], which is why we see the calibrated model adapts by decreasing the value of the COP of the equipment accompanied with the sudden drop of heating input of Fig. 17.

The results for the auxiliary air loop show a parallel of this decrease in the performance for the AHU's DX heating coil under

Table 17
Comparison of parameter values between the Baseline BEM and the Calibrated BEM after the calibration process of the Air Handling Unit and it's expansion coil for the Winter Training Period 2019–2020.

Equipment	Component	Parameter	Units	Baseline Model	Calibrated Model
AHU	Air to Air	Nominal Supply Air Flow Rate	m^3/s	0.5555560	0.4680955
	Heat	Sensible Effectiveness at 100% Heating Air Flow	–	0.80	0.25
	Exchanger	Latent Effectiveness at 100% Heating Air Flow	–	0.73	0.50
		Sensible Effectiveness at 75% Heating Air Flow	–	0.83	0.70
		Latent Effectiveness at 75% Heating Air Flow	–	0.74	0.85
	Heating	Gross Rated Total Heating Capacity	W	10000	6576
	DX Coil	Gross Rated Heating COP	W/W	3.34	1.50
		Rated Air Flow Rate	m^3/s	0.6030000	0.5299012
	Heating	Total Heating Capacity Function of Temperature Curve Name			
	DX Coil	Coefficient C1	–	0.7577494	0.6982403
		Coefficient C2	–	0.0275897	0.0259275
		Coefficient C3	–	0.0001485	0.0001420
		Coefficient C4	–	0.0000035	0.0000029
	Heating	Energy Input Ratio Function of Temperature Curve Name			
	DX Coil	Coefficient C1	–	1.1916933	1.2922829
		Coefficient C2	–	−0.0300239	−0.0292722
		Coefficient C3	–	0.0010368	0.0007603
		Coefficient C4	–	−0.0000233	−0.0000229

these winter conditions. Here the coil's heating capacity has dropped from 10.00 kW to 6.58 kW a 34.2% and the coils CoP decreased 55.1% to 1.50 as displayed in Table 17.

The only difference between the AHU DX heating coil and the VRF outdoor unit lies in the use of cubic equations to define the performance curves on the DX Coil rather than the usual bi-quadratic, an option that only links outdoor temperature with heating performance and power consumption. As Fig. 18 shows, for the AHU DX heating coil there is little difference between the calibrated curve and the baseline model one.

The difficulty of finding the parameter values through the calibration process may be seen on Fig. 19, where the baseline model cluster displayed in yellow has a general slope that is closer to the horizontal than to the 45° optimal line. This means the baseline equipment is not even remotely operating as intended. This results in a longer iterative process, cycling multiple times through the flow of the diagram shown in Fig. 1 in order to reduce the dispersion of the simulated solutions and fix the alignment (rotation) of the cluster. In other words making the simulation model behave as intended.

In terms of energy consumption, there is a clear improvement between the baseline model and the BEM that undergoes the calibration process. The Cv(RMSE) shown in Table 18 is 27.18% and well within ASHRAE standard; while for NMBE, the BEM reaches a 10.23% just barely above the threshold permitted by the international standard. As for the goodness-of-fit R^2 coefficient although the calibrated BEM remains below 75% value recommended by the standards, there is an increment of over 50% from the baseline model results. This increment can also be seen in the dispersion graph on Fig. 19, where the cluster of hourly points of the model that undergoes the calibration process (in blue) seem to realign with the 45° optimal line.

The results from this partially calibrated model are obtained while maintaining indoor conditions, as Table 19 shows, where we obtain an average RMSE for the whole building of 0.462 °C with an average R^2 of 93.966%. It is to be noted that these indoor conditions are maintained by a building energy model whose HVAC system has a reduced value for heating capacity across all of its different components, suggesting the work ratio of the system under those particular conditions to keep those indoor temperatures fixed.

When the assessing the results obtained for this particular 2019-20 winter campaign, there is a clear gap between the simulation model and the real HVAC installation energy performance. The VRF system that meets the building's heating demand seems to be working under extremely unfavorable conditions primarily influenced by the test site's "warm" winter weather. On VRF installations, the site's outdoor conditions not only affects the equipment efficiency parameters, since it also affects the building's heating demand, it forces the HVAC system to operate at a non optimal part load ratio. In other words this results are a demonstration of how a design gap works.

What we have seen during this whole process is an HVAC system whose main focus is to provide cooling into the building spaces. In other words a system that has been designed for summer conditions, and given the weather of the site, the amount of operational hours obtained for summer and winter, and the results of the calibration process, this may very well be the case. The installed unit seems to be oversized for winter conditions, or at least it is oversized for the particular conditions of winter 2019-20, which makes the unit work at a low part load ratio and/or under weather conditions that penalize the systems efficiency.

This adds a new layer of difficulty when calibrating a BEM model, as seen with the heating operation of the VRF system, where the equipment installed in the building normally operates well below it's optimal range and that makes simulation model struggle to find a solution that fits into reality. This difference in the behaviour and energy performance of the equipment between heating and cooling operation modes may be the reason that in some cases it seems more difficult to meet calibration requirements in one operating condition than on the other.

5. Conclusions

The methodology applied have allowed us to produce a model that takes into account all of the building's systems, from it's envelope to its detail HVAC components. Furthermore, the evaluation of this VRF model under multi level benchmark of indoor temperature and electric consumption allow us to capture: the buildings thermal dynamics, it's HVAC system thermal energy performance and electric consumption. The results in electric consumption are obtained while maintaining indoor temperature in each TZ which

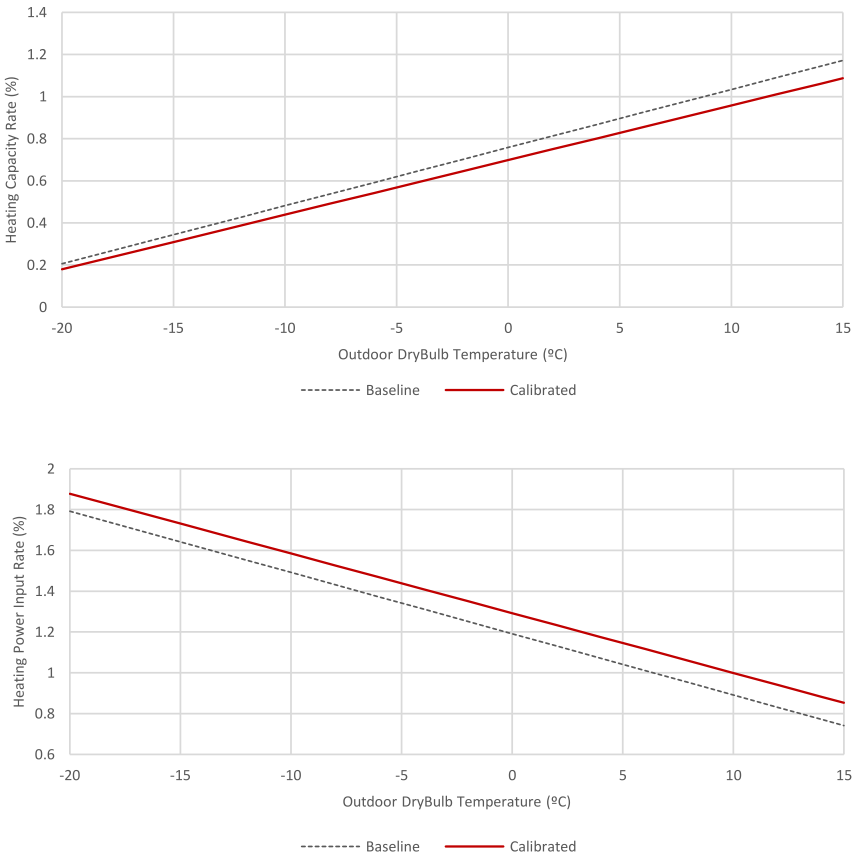

Fig. 18. Heating Coil performance curves for the AHU DX Heating Coil component: Heating Capacity (above) and Heating Input (below) generated for the Baseline Model (obtained from DB technical library for a similar equipment) displayed in black and for the Calibrated Model obtained after the optimization process displayed in red. (For interpretation of the references to colour in this figure legend, the reader is referred to the web version of this article.)

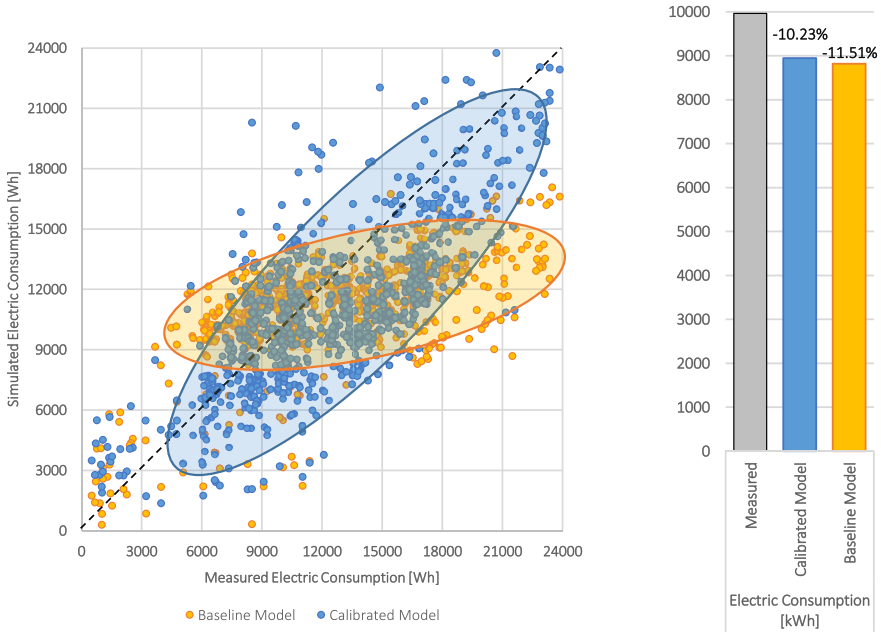

Fig. 19. Performance results for electric consumption of the calibrated BEM for the heating calibration period from November 2019 to April 2020.

Table 18
Electric Consumption hourly uncertainty index for the Heating Calibration period using 802 hours of operation between November 2019 to April 2020.

	International Standard		Electric Consumption Results	
INDEX	ASHRAE	IMPVP	Baseline Model	Calibrated Model
NMBE	±10%	±5%	11.513%	10.234%
Cv(RMSE)	30%	20%	32.497%	27.180%
R^{2a}	75%	75%	38.284%	59.473%

[a]Although there is no universal standard for a minimum acceptable R^2 threshold, values above 75% are often considered a sign of a good causal relationship amongst the energy and independent variables.[16].

Table 19
Indoor thermal zone temperature hourly uncertainty index for the Heating Calibration period using 802 hours of operation between November 2019 to April 2020.

	Indoor Temperature by TZ							Building
INDEX	Tz-02	Tz-03	Tz-04	Tz-08	Tz-09	Tz-10	Tz-11	Average
MAE (°C)	0.170	0.056	0.036	0.375	0.256	0.262	0.397	0.194
RMSE (°C)	0.705	0.198	0.099	0.931	0.763	0.688	0.966	0.462
NMBE (%)	0.699	−0.087	−0.030	1.462	0.980	0.827	1.558	0.712
Cv(RMSE) (%)	3.150	0.968	0.410	4.109	3.171	3.084	4.413	2.086
R^2 (%)	89.474	99.056	99.715	86.797	91.013	82.361	73.875	93.966

can only mean that we have indirectly captured the thermal energy performance of the VRF system through the optimization of it's performance curve values and that the resulting thermal energy is being distributed correctly through the building. Generating a BEM with high quality results, as displayed in Section 4.1, using 1717 hours for it's training period. A model stable through time as demonstrated on Section 4.2, one year apart, fitting into 2077 hours of operation.

Moreover, as the winter scenario in Section 4.3 shows, this calibration process greatly improves the results of a BEM when compared against it's baseline counterpart. The application of this methodology and working with "families" of solutions regarding VRF curve and parameter relationship allow us to correct the behavior of the baseline model during winter to closely match the performance of the equipment using only 802 hours of data as training. The obtained partially calibrated BEM model has clearly demonstrate the design gap of the equipment and established the normal operation range of the HVAC system during 2019-20 winter season to be inefficient. In addition, the results of the process allowed us to point out some of the main reasons why the equipment behaves as it does: local weather conditions far warmer than expected, and possible oversize of the heating side due to the fact that the VRF system main design objective is cooling demand.

Which furthers reinforce the idea that regardless of how good a baseline model has been developed to represent the actual building and its installed HVAC systems; even if all of its parameters are set to nominal or known values obtained from the best technical specifications available, it may be performing under unfavorable conditions or the building systems may have design gaps, and therefore it is unavoidable to always execute a calibration of a BEM.

Future studies will focus on refining and expanding the application of this methodology, performing validations into other buildings with different configurations of HVAC systems, testing it's flexibility and adapting it to a variety of different scenarios. Researching the amount of hours required to achieve calibration and aiming to further develop it into a tool that could be applied to develop BEM with advance capabilities as a tool for Fault Detection Diagnosis (FDD) or Model Predictive Control (MPC).

Funding

The researchers Carlos Fernández Bandera and Jose Pachano have been funded by the Government of Navarra under the project "From BIM to BEM: B&B" (ref. 0011-1365-2020-000227).

CRediT authorship contribution statement

José Eduardo Pachano: Conceptualization, Methodology, Software, Validation, Investigation, Writing – original draft, Writing – review & editing. **Antonis Peppas:** Supervision. **Carlos Fernández Bandera:** Conceptualization, Methodology, Software, Validation, Investigation, Resources, Writing – review & editing, Supervision, Project administration, Funding acquisition.

Declaration of Competing Interest

The authors declare that they have no known competing financial interests or personal relationships that could have appeared to influence the work reported in this paper.

Acknowledgments

We would like to thank NTUA (Greece), the EU project H2020 SABINA (Grant No. 731211) for providing us with both the building documentation and the sensor data to perform the necessary tests for this paper.

References

[1] T.N. Aynur, Variable refrigerant flow systems: A review, Energy Build. 42 (2010) 1106–1112.
[2] D. Kim, S.J. Cox, H. Cho, P. Im, Model calibration of a variable refrigerant flow system with a dedicated outdoor air system: A case study, Energy Build. 158 (2018) 884–896.
[3] D. Zhao, X. Zhang, M. Zhong, Variable evaporating temperature control strategy for vrv system under part load conditions in cooling mode, Energy Build. 91 (2015) 180–186.
[4] H.A. Gilani, S. Hoseinzadeh, H. Karimi, A. Karimi, A. Hassanzadeh, D.A. Garcia, Performance analysis of integrated solar heat pump vrf system for the low energy building in mediterranean island, Renew. Energy 174 (2021) 1006–1019.

[5] K. Chua, S. Chou, W. Yang, J. Yan, Achieving better energy-efficient air conditioning – a review of technologies and strategies, Appl. Energy 104 (2013) 87–104.
[6] J.H. Lee, H. Kim, Y. hak Song, A study on verification of changes in performance of a water-cooled vrf system with control change based on measuring data, Energy Build. 158 (2018) 712–720..
[7] T.N. Aynur, Y. Hwang, R. Radermacher, Simulation comparison of vav and vrf air conditioning systems in an existing building for the cooling season, Energy Build. 41 (2009) 1143–1150.
[8] X. Yu, D. Yan, K. Sun, T. Hong, D. Zhu, Comparative study of the cooling energy performance of variable refrigerant flow systems and variable air volume systems in office buildings, Appl. Energy 183 (2016) 725–736.
[9] I. Promoting, Energy efficiency investments. case studies from the residential sector, Paris: International Energy Agency and Agence Francaise de Development (2008)..
[10] A. Clerici, G. Alimonti, World energy resources, in: EPJ Web of Conferences, volume 98, EDP Sciences, p. 01001..
[11] E.C. Prices, Co2 emissions from fuel combustion international energy agency (????)..
[12] L. Pérez-Lombard, J. Ortiz, C. Pout, A review on buildings energy consumption information, Energy Build. 40 (2008) 394–398.
[13] I.C. Change et al., Mitigation of climate change, Contribution of Working Group III to the Fifth Assessment Report of the Intergovernmental Panel on, Clim. Change 1454 (2014).
[14] D. Coakley, P. Raftery, M. Keane, A review of methods to match building energy simulation models to measured data, Renew. Sustain. Energy Rev. 37 (2014) 123–141.
[15] U. Doe, M&v guidelines: measurement and verification for federal energy projects version 3.0, US Department of Energy (2008).
[16] I. Committee, et al., International Performance Measurement and Verification Protocol: Concepts and options for determining energy and water savings, Volume I, Technical Report, National Renewable Energy Lab., Golden, CO (US), 2001..
[17] ASHRAE, Ashrae guideline 14-2002: measurement of energy and demand savings, ASHRAE Guide 8400 (2002) 1–165..
[18] M. Yasin, E. Scheidemantel, F. Klinker, H. Weinläder, S. Weismann, Generation of a simulation model for chilled pcm ceilings in trnsys and validation with real scale building data, J. Build. Eng. 22 (2019) 372–382.
[19] D. Monfet, R. Zmeureanu, Calibration of a central cooling plant model using manufacturer's data and measured input parameters and comparison with measured performance, J. Build. Performance Simul. 6 (2013) 141–155.
[20] A. Mihai, R. Zmeureanu, Bottom-up evidence-based calibration of the hvac air-side loop of a building energy model, J. Build. Performance Simul. 10 (2017) 105–123.
[21] G.L. Martin, D. Monfet, H.F. Nouanegue, K. Lavigne, S. Sansregret, Energy calibration of hvac sub-system model using sensitivity analysis and meta-heuristic optimization, Energy Build. 202 (2019) 109382.
[22] P. Raftery, M. Keane, J. O'Donnell, Calibrating whole building energy models: An evidence-based methodology, Energy Build. 43 (2011) 2356–2364.
[23] Z. Yang, B. Becerik-Gerber, A model calibration framework for simultaneous multi-level building energy simulation, Appl. Energy 149 (2015) 415–431.
[24] D.E. Claridge, Using simulation models for building commissioning (2004)..
[25] R. Escandón, R. Suárez, J.J. Sendra, On the assessment of the energy performance and environmental behaviour of social housing stock for the adjustment between simulated and measured data: The case of mild winters in the mediterranean climate of southern europe, Energy Build. 152 (2017) 418–433.
[26] G.R. Ruiz, C.F. Bandera, Analysis of uncertainty indices used for building envelope calibration, Appl. Energy 185 (2017) 82–94.
[27] G.R. Ruiz, C.F. Bandera, T.G.-A. Temes, A.S.-O. Gutierrez, Genetic algorithm for building envelope calibration, Appl. Energy 168 (2016) 691–705.
[28] D. Zhang, X. Zhang, J. Liu, Experimental study of performance of digital variable multiple air conditioning system under part load conditions, Energy Build. 43 (2011) 1175–1178.
[29] D. Guyot, F. Giraud, F. Simon, D. Corgier, C. Marvillet, B. Tremeac, Building energy model calibration: A detailed case study using sub-hourly measured data, Energy Build. 223 (2020) 110189.
[30] R.A. Lara, E. Naboni, G. Pernigotto, F. Cappelletti, Y. Zhang, F. Barzon, A. Gasparella, P. Romagnoni, Optimization tools for building energy model calibration, Energy Proc. 111 (2017) 1060–1069. 8th International Conference on Sustainability in Energy and Buildings, SEB-16, 11-13 September 2016, Turin, Italy..
[31] W. Li, Z. Tian, Y. Lu, F. Fu, Stepwise calibration for residential building thermal performance model using hourly heat consumption data, Energy Build. 181 (2018) 10–25.
[32] A. Cacabelos, P. Eguía, L. Febrero, E. Granada, Development of a new multi-stage building energy model calibration methodology and validation in a public library, Energy Build. 146 (2017) 182–199.
[33] B. Merema, M. Delwati, M. Sourbron, H. Breesch, Calibration of a bes model of an educational building with demand controlled ventilation, in: 15th conference of IBPSA 43, vol. 51..
[34] G.Y. Yun, K. Song, Development of an automatic calibration method of a vrf energy model for the design of energy efficient buildings, Energy Build. 135 (2017) 156–165.
[35] W.H. Kang, J.M. Lee, S.H. Yeon, M.K. Park, C.H. Kim, J.H. Lee, J.W. Moon, K.H. Lee, Modeling, calibration, and sensitivity analysis of direct expansion ahu-water source vrf system, Energy 199 (2020) 117435.
[36] R. Yin, S. Kiliccote, M.A. Piette, Linking measurements and models in commercial buildings: A case study for model calibration and demand response strategy evaluation, Energy Build. 124 (2016) 222–235.
[37] M. Hydeman, K.L. Gillespie, A. Dexter, Tools and techniques to calibrate electric chiller component models, ASHRAE Trans. 108 (2002) 733–741.
[38] J. Stein, M.M. Hydeman, Development and testing of the characteristic curve fan model, ASHRAE Trans. 110 (2004).
[39] T. Hong, J. Kim, J. Jeong, M. Lee, C. Ji, Automatic calibration model of a building energy simulation using optimization algorithm, Energy Proc. 105 (2017) 3698–3704. 8th International Conference on Applied Energy, ICAE2016, 8–11 October 2016, Beijing, China..
[40] J. Chen, X. Gao, Y. Hu, Z. Zeng, Y. Liu, A meta-model-based optimization approach for fast and reliable calibration of building energy models, Energy 188 (2019) 116046.
[41] A. Chong, K. Menberg, Guidelines for the bayesian calibration of building energy models, Energy Build. 174 (2018) 527–547.
[42] H. Lim, Z.J. Zhai, Influences of energy data on bayesian calibration of building energy model, Appl. Energy 231 (2018) 686–698.
[43] J.E. Pachano, C.F. Bandera, Multi-step building energy model calibration process based on measured data, Energy Build. 252 (2021) 111380.
[44] V. Gutiérrez González, G. Ramos Ruiz, C. Fernández Bandera, Empirical and comparative validation for a building energy model calibration methodology, Sensors 20 (2020) 5003.
[45] H. Torio, A. Angelotti, D. Schmidt, Exergy analysis of renewable energy-based climatisation systems for buildings: A critical view, Energy Build. 41 (2009) 248–271.
[46] A. Entrop, H. Brouwers, Ecbcs annex 49 (????)..
[47] Y. Zhang, I. Korolija, Performing complex parametric simulations with jeplus, in: SET2010-9th International Conference on Sustainable Energy Technologies, pp. 24–27..
[48] K. Deb, A. Pratap, S. Agarwal, T. Meyarivan, A fast and elitist multiobjective genetic algorithm: Nsga-ii, IEEE Trans. Evol. Comput. 6 (2002) 182–197.
[49] The Chartered Institution of Building Services Engineers, Requirements to be met by calculation methods for the simulation of thermal-energy efficiency of buildings and building installations, Standard ISBN978-1-912034-76-5, The Chartered Institution of Building Services Engineers, 222 Balham High Road, London SW12 9BS, 2020..
[50] M. Royapoor, T. Roskilly, Building model calibration using energy and environmental data, Energy Build. 94 (2015) 109–120.
[51] VDI-Fachbereich Technische Gebäudeausr++stung, Requirements to be met by calculation methods for the simulation of thermal-energy efficiency of buildings and building installations, Standard DINGCD22, Verlag des Vereins Deutscher Ingenieure, VDI - Platz 1, D++sseldorf, 40468 Germany, 2001..
[52] V.G. González, L.Á. Colmenares, J.F.L. Fidalgo, G.R. Ruiz, C.F. Bandera, Uncertainty's indices assessment for calibrated energy models, Energies 12 (2019) 2096.
[53] C. Beck, J. Grieser, M. Kottek, F. Rubel, B. Rudolf, Characterizing global climate change by means of köppen climate classification, Klimastatusbericht 51 (2005) 139–149.
[54] E.L. Segarra, G.R. Ruiz, V.G. González, A. Peppas, C.F. Bandera, Impact assessment for building energy models using observed vs. third-party weather data sets, Sustainability 12 (2020).
[55] H. Lim, Z.J. Zhai, Comprehensive evaluation of the influence of meta-models on bayesian calibration, Energy Build. 155 (2017) 66–75.
[56] U. DoE, Energyplus engineering reference, The reference to energyplus calculations (2010)..
[57] AHRI Air-Conditioning, Heating and Refrigeration Institute, Performance Rating of Central Station Air-Handling Units, Standard 430, AHRI Air-Conditioning, Heating and Refrigeration Institute, 2111 Wilson Boulevard Suite 500, Arlington, VA 22201, USA, 2009..
[58] D. Zhou, S.H. Park, Simulation-assisted management and control over building energy efficiency–a case study, Energy Proc. 14 (2012) 592–600.
[59] Y. Pan, Z. Huang, G. Wu, Calibrated building energy simulation and its application in a high-rise commercial building in shanghai, Energy Build. 39 (2007) 651–657.
[60] D. Coakley, P. Raftery, P. Molloy, G. White, Calibration of a detailed bes model to measured data using an evidence-based analytical optimisation approach, Proc. Build. Simul. 2011 (2011).
[61] Y.-S. Kim, M. Heidarinejad, M. Dahlhausen, J. Srebric, Building energy model calibration with schedules derived from electricity use data, Appl. Energy 190 (2017) 997–1007.
[62] E. Lucas Segarra, H. Du, G. Ramos Ruiz, C. Fernández Bandera, Methodology for the quantification of the impact of weather forecasts in predictive simulation models, Energies 12 (2019) 1309.
[63] G. Ramos Ruiz, E. Lucas Segarra, C. Fernández Bandera, Model predictive control optimization via genetic algorithm using a detailed building energy model, Energies 12 (2019) 34.
[64] E. Lucas Segarra, G. Ramos Ruiz, C. Fernández Bandera, Probabilistic load forecasting for building energy models, Sensors 20 (2020) 6525.